

Industrial looks at ways of manufacturing defects of fiber reinforced polymer composites.

Lijin Kottayil Raghavan

A thesis submitted to the graduate faculty in partial fulfillment of the requirements for the degree
of MASTER OF SCIENCE

Major: Industrial Engineering

Program of Study Committee:

Frank Peters, Major Professor

Matthew Frank

Vinay Dayal

Iowa State University

Ames, Iowa

2014

Copyright © Lijin Kottayil Raghavan, 2014. All rights reserved

List of Contents

List of Figures.....	03
List of Tables.....	06
Acknowledgments.....	07
Abstract.....	08
Chapter 1. Introduction	09
Chapter 2. Literature Review.....	12
Fabric Manipulation/shifting.....	12
Fabric Layup and Resin infusion.....	18
Compressive testing and failure.....	21
Fatigue cycle testing and Failure.....	23
Chapter 3. Research Goal.....	27
Chapter 4. Methodology.....	28
Shear-lock limit.....	28
Experimental Design.....	30
Test setup- making of coupons, geometry, equipment used.....	32
Compressive Testing and Compressive-Fatigue Testing	33
Chapter 5. Results and Discussions.....	38
Chapter 6. Conclusions and Future works.....	48
Future work.....	50
References.....	52
Appendix.....	56

List of Figures

- Figure 01: The process of shifting mechanism on the fabric explained [38]
- Figure 02: Unidirectional Fabric and Terms [39]
- Figure 03: Explanation on the Shifting of Fabric [39]
- Figure 04: In-plane Waviness and Out-of-plane Waviness in Composite Laminates [2]
- Figure 05: Laminate with Introduced Waviness (left) and Waviness Characterization (Right) [40].
- Figure 06: IP waves imparted into a layer in a 0° laminate (left) and an OP wave form used to impart necessary wave into a 0° laminate (right) [41].
- Figure 06: (a) Representative volume and coordinates for a unidirectional composite with uniform waviness (b) Representative volume and coordinates for a unidirectional composite with graded waviness [17]
- Figure 08: (a) Layer by layer in-plane flaw by radiography. (b) Out of plane defects identification by radiography
- Figure 09: (a) Tow thinning seen in a fabric on shifting 35° (b) Out of plane defects identification visual inspection for 25° Shifted fabric.
- Figure 10: Geometries of imperfection considered in a unidirectional fiber composite: (a) an infinite band of waviness; (b) a circular patch of waviness, and (c) a beam containing a parallel-sided band of waviness under bending [21]
- Figure 11: Micro-buckling Failure of a Wavy Composite Laminate Subjected to Compressive Loads [22]
- Figure 12: Schematic edge views of damage morphologies in two layer PW GFRP laminates [42]
- Figure 13: Deformed meshes for staggered geometry with increasing number of layers in model and crack located adjacent to crimp: [a] two layer; [b] four layer; [c] infinitely thick.
- Figure 14: (a) Static Compression Failure Mode for a Typical Unidirectional Fabric for the 0° Plies, (b) Compression Failures for Glass Fiber Laminates Containing Induced In-Plane Waviness [40]
- Figure 15: Alignment of Kink Band with respect to Longitudinal Axis [12]
- Figure 16: Typical Comparison of Metal and Composite Fatigue Damage
- Figure 17: Schematic of Edge Splitting in Unidirectional Materials [35]
- Figure 18: Fatigue Failure Modes for Composite Materials [38]

Figure 19: Schematic representation of the development of damage during the fatigue life of a composite laminate [43].

Figure 20: Schematic representation of the shear lock limit within fabric tows [44]

Figure 21: [a] Shear lock limit testing setup; [b] The shear lock limit measuring on an unidirectional fabric

Figure 22: The fabric Shifting Machine at Iowa State University.

Figure 23: Resin infusion process to create the 4 layered sample.

Figure 24: Cross sectional view of the resin infusion setup [39]

Figure 25: (a) Graphical representation of the sample after infusions and the coupon location (b) Coupon structure and orientation

Figure 26: (a) Instron 8801 compression and fatigue testing machine used in the study (b) Instron 3580 Hydraulic power unit

Figure 27: (a) Schematic of Compression Test Fixture [45], (b) Actual jaw and head of the testing machine

Figure 28: Schematic Illustrating Compressive Cyclic Loading

Figure 29: Compression Test Specimen Three-Part Failure Identification Codes and Overall Specimen Failure Schematics [45]

Figure 30: Schematic representation of tow thinning due to varying radius of curvature within bunch of fiberglass in a tow.

Figure 31: Schematic representation of the side of coupon depicting the cause of roughness due to fiber orientation after shifting.

Figure 32: A graphical representation of change in average coupon thickness versus change in average compressive force

Figure 33: A comparison between tows in a shifted coupon versus average compressive strength of shifted coupon - Data from *table 02*.

Figure 34: Compression results of the Straight Coupon cut from the shifted sample versus shifted coupons cut from shifted samples

Figure 35: Strength Analysis on a coupon with lower out-of-plane [7 inch radius of curvature] waviness.

Figure 36: Strength Analysis on a coupon with higher out-of-plane [4 inch radius of curvature] waviness

Figure 38: A comparison between compression test data [Average Compressive Strength] versus shift angle and Fatigue cycle data [Average Fatigue Cycles] versus shift angle

List of tables

Table 01: Strength Summary for the straight coupon cut from shifted sample

Table 02: Compression test result for shifted coupon from two trials

Table 03: Fatigue testing results of the samples- Load applied and number of cycles sustained.

Acknowledgements

I have been a graduate student at Iowa State University for 2 years and it was a great honor and experience for me to work and take classes with notably: Dr. Frank Peters and Dr. Matthew Frank. First I want to thank Dr. Frank Peters, my major advisor for his guidance, master idea and opportunity for this thesis and encouragement through my graduate career. Without his constant assistance it would be impossible for me to finish this research work. I also want to thank Dr. Matthew Frank and Dr. Vinay Dayal for serving as my graduate committee members for giving me right directions towards completing my thesis. I also want to mention a special thanks to Dr. Vinay Dayal for providing me with research materials and critical ideas throughout the research work.

I specially acknowledge Siqi Zhu, Sunil Chakrapani and Wyman Martinek for their assistance in laboratories towards experimental research. I would like to thank my parents who gave me all the support and help throughout my education.

Abstract

This study investigates the effect of fabric manipulation on performance of unidirectional non-crimp fiber reinforced polymer composites. Conventionally hand layup process is being followed in wind turbine manufacturing industries which is a time consuming process. To overcome the long man labor, automatic layup method could be used to make the process faster. Before implementing the automatic layup process in industries, it is essential to study how in-plane wave caused by shifting is going to affect the properties of the fabric and thus predict the life of the fabric. Fatigue and compressive tests were conducted on the fabric to study the behavior of the fabric in actual wind turbine manufacturing applications.

Samples were made by stacking four layers of fabric one over each other with a definite shift angles and then followed by resin infusion and then cut the coupons for testing. Stacking of in-plane wave samples over each other resulted in formation of out of plane waviness. Eight coupons per shift angles of 5, 10, 15, 20 and 25 degree were cut out for tests. Compression loading and compression fatigue testing was performed on the samples to characterize the properties.

The maximum strength level concentration acted on the point of grip on the fabric sample. The result from the experimental tests support and help explain the impact of shifting on the unidirectional fiber reinforced polymer composites and used to establish the manufacturing defects in the unidirectional fabric from shifting process.

Chapter 1: Introduction

In wind turbine manufacturing industries, conventional hand lay-up of fabric is labor extensive and have several other problems and results in uneven shear and strength distribution. The uneven and undesired shear distributions results in weakened mechanical properties, extensive rework and scrapping of the materials. Shifting is the process of manipulating the fabric tows perpendicular to the fiber direction. Instead of steering, shifting of fabric to create in-plane wave is adopted by the machine used in this research. In-plane waviness caused by the shifting machine was the key point in this study. The shifting machine is a set up for holding the fabric along one of the fiber directions and “sliding” the free end parallel to the hold in order to change the direction of the fiber [38]. This can be thought of as similar to deforming a rectangle into a parallelogram. These deformed fabric layers were stacked in fours over each other to make a sample. The shifting of fabric which results in in-plane waviness affects the compressive and fatigue life of the composite materials. Difference in compressive strength between coupons with varying shift angles were studied.

Shifting of fabric can cause high potential loss of material property. This work investigated on the effects of such shifting affecting the level of manufacturing quality of reinforced polymer composites. The amount of acceptable deviations varies from applications to application, however there is no criterion that enables the regulations or guidelines to be laid for a structure with wavy plies. The findings from the thesis enable to define a performance acceptance of fiber reinforced polymer composites. A study of ply localized waviness by the fabric shifting machine in a unidirectional composite fabric is carried out in this thesis.

Creating in-plane shift optimized fabrics by individual tow placement by shifting mechanism will provide a process of controlling the shift distribution without involving many workers. A better practical application for process control would be to change the shift angle distribution of the unidirectional fabric to the desired alignment prior to lay-up [44]. A guide for

automatic deposition of fabric into a curved path using an incremental shift of a portion of fabric in the weft direction was developed by Magnussen [38]. Doing so will require minimal or no smoothing work on the laid fabric. The process of shifting mechanism to the fabric can be better understood in the *figure 01*.

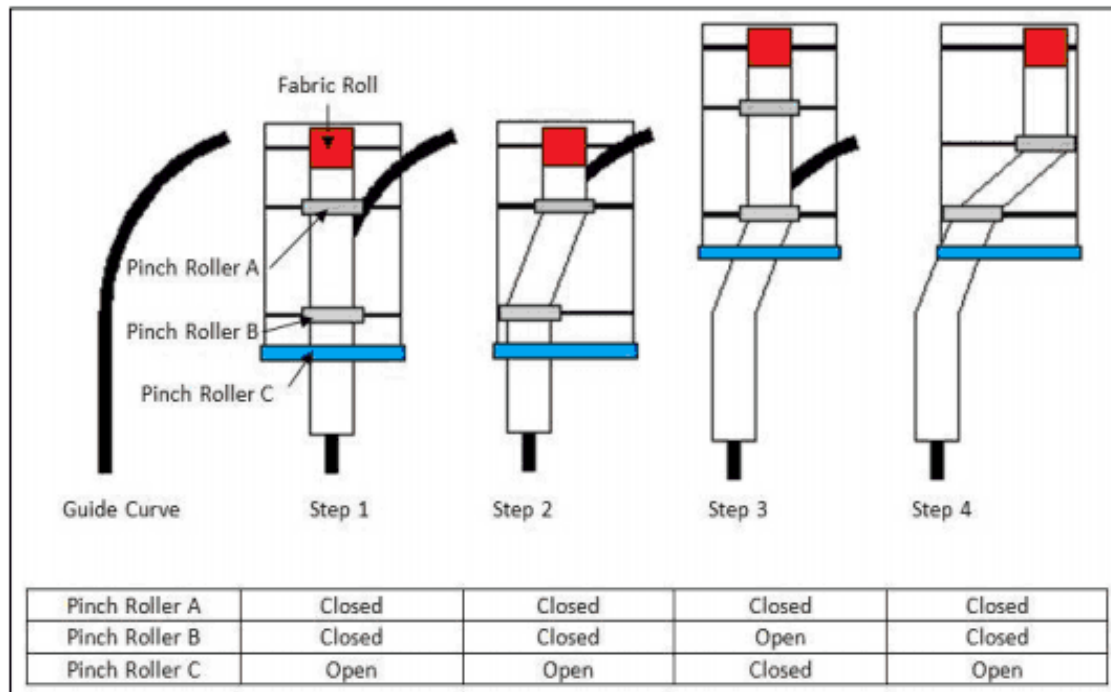


Figure 01: The illustration of shifting mechanism on the fabric [38]

Shifting of fabric causes in-plane waviness and in order to understand the effect of waviness of plies, characterization of waviness is essential. The research begins with characterizing the straight fabric using compressive and fatigue tests and based on that, the shifted fabrics are compared. Fatigue and compressive tests done on the fabric coupons create a common understanding of the fabric behavior under various loading conditions. The characterized study of failure under an idealized versus waviness condition will create a better understanding of the effects of waviness. In this thesis, analytical and numerical based finite element analyses have been carried out to understand the effects of wave plies in a composite laminate subjected to compressive loads which reveals about the strength concentrations. The purpose of the finite element analysis is to create the sample model and to determine the

possible regions of failure in the laminate and predict the failure modes and strength. The mechanical tests helps us to understand the effects of waved plies in composite laminates for shift angles above 10 degrees.

Waviness which are a common occurrence in composite materials could be either unintentionally induced into composites during processing, or inherent in the fiber orientation. The unintentionally induced waviness is classified as two types: one is in-plane waviness or fiber waviness, the other is out-of-plane waviness. Both of them may be induced by fabric layup and infusion processes and may also be the result of residual thermal strengthes that are caused by the different thermal expansion rates between fiber and matrix materials [1]. Fabrics when shifted causes in-planes waviness, but exceeding the shift angle beyond a certain limit results in out-of-plane waviness, cross tow breakage and tow thinning.

Except the fabric shift angles, parameters of compression and fatigue tests, its setup were kept constant to focus the effect of shift on the fabric. Extreme care has been taken while making samples and coupons to get consistent sample geometry in order to prevent any other parameters to influence the findings. Effects of compressive strength and fatigue cycle count on shifted fabric were analyzed. The result of findings from mechanical tests helped in understanding the effects of in- plane waviness caused by shifting on unidirectional [Figure 02] NCF fabric composite material.

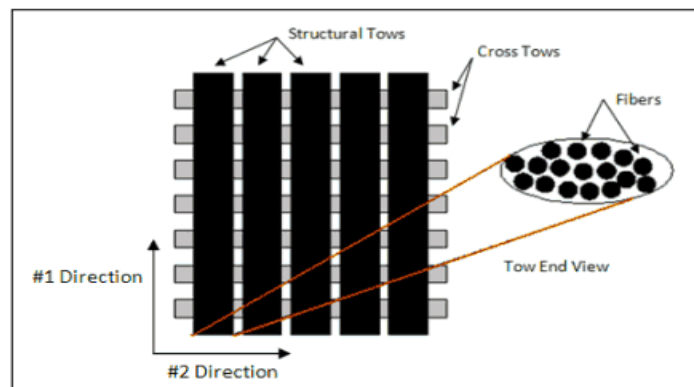


Figure 02: Unidirectional Fabric and Terms [39]

Chapter 2: Literature Review

Fabric Manipulation/Shifting

Fabric hand layup process is also known as the fabric draping process. Several studies have been conducted on draping and manipulation processes and its effect on fiberglass properties. Automatic fabric shifting machine is used for this study and before this automated draping process is adopted for production it is important to study its impact on fabric properties. Automated tape layup precisely places narrow “tapes” of pre-impregnated composite onto the surface of a mold; however, this process is expensive in manufacturer point of view considering the equipment cost, the input materials and extensive time consumption [46]. Several other researches have been made to automate the fabric layup process. A robot capable replacing the hand layup by acquiring the fabric and then placing it on the mold, stacking and finally smoothing of the stacking has been proposed by Ruth [47]. A similar study has been done by Sarahidi [48] wherein electrostatic pins grabs the fabric by hooking it, then placing the fabric in desired mold location and then flattening it. It also had a vision system to ensure the fabric is flat on placing it in mold.

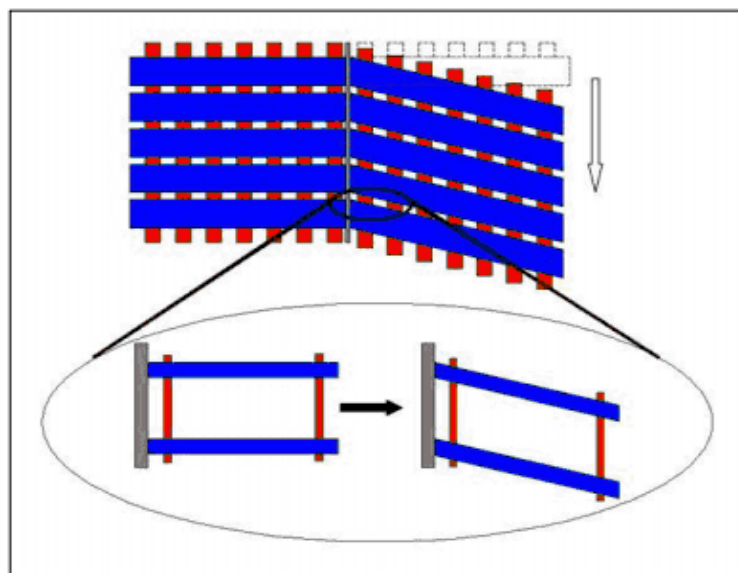


Figure 03: Explanation on the Shifting of Fabric [39]

Waviness can be either unintentionally induced into composites during processing, or inherent in the fiber architecture. The induced waviness into fabric is classified as two types: in-plane waviness and out-of-plane waviness. In-plane waviness, or fiber waviness, describes the fiber deviations from straight 0 degree in the plane of the fabric sheet. Out-of-plane waviness, or layer waviness, involves layers of a multidirectional laminate undulating in the through-thickness direction. The two types of waviness are illustrated in *figure 04*. Experimental results [6] show that draping does significantly change orientation, fiber volume fraction, permeability thus affecting the resin flow rate. Pin jointed net (PJN) model fabric were used for the study and is assumed to be inextensible, and the joint between different fiber directions is represented as a pin. The angle between fibers at these pins is then changed to deform the fabric. The angle between the tows is referred to as the shear angle. This has been shown to describe the behavior and deformability of the fabric well [3]. When the fabric reaches its maximum allowable angle – its shear locking limit (SLL) – it will buckle resulting in out-of-plane waviness. According to Potter [3], out-of-plane waviness has to occur considering the reduction of fabric width on shifting the fabric. Reduction in fabric width is caused when the tow thinning is narrowed down when the fiberglass within the tows are overlapped due to the shifting and deformation.

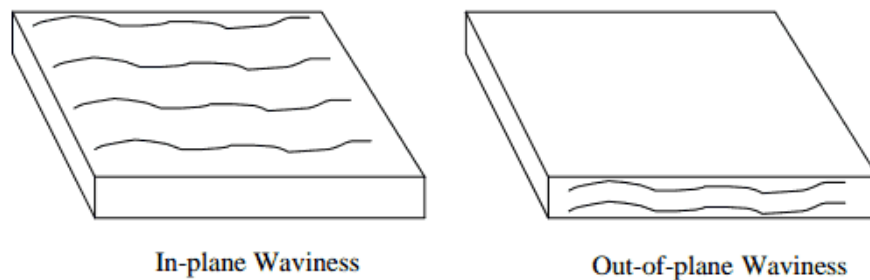


Figure 04: In-plane Waviness and Out-of-plane Waviness in Composite Laminates [2]

The shifting of the fabric is followed by resin transfer to make the samples and then cut coupons out of it for testing. The shifted fabric were placed in the mold for resin infusion. Once

the mold has been sealed, a polymeric resin is infused into the mold cavity, saturating the preform and expelling any air present, a curing reaction is initiated, usually after complete filling of the mold cavity, and the part solidifies. The finished composite product can then be removed from the mold [5].

The effect of strength reductions in laminates due to in-plane waviness [Figure 05] were initially studied and explored by Joyce and Moon [16]. They found that the strength reductions due to in plane waviness produces similar effects to that of laminates that fail due to strength concentration. An analytical model was developed by Bogetti [15] to study the effects of ply waviness in a cross ply laminate. The model in the study was developed to predict the effects on the strength and stiffness reduction due to in-plane waviness in a composite laminate. The amount of strength deteriorating and the ply failure due to waviness was explained in his studies. One of his major principal findings was the strength reduction from inter laminar shear failure. Tows in the area of in-plane waves are denser because fiberglass within each tows are overlapped due to the shifting force. The overlapping of fiberglass reduced the tow width, but increases the tow thickness. When the fabrics with in-plane wave are stacked by overlapping the in-plane fabric, it result in out of plane wave due to the tow thickness. This phenomenon is seen in figure 9 and is also clearly depicted by Riddle [41] (Figure 06).

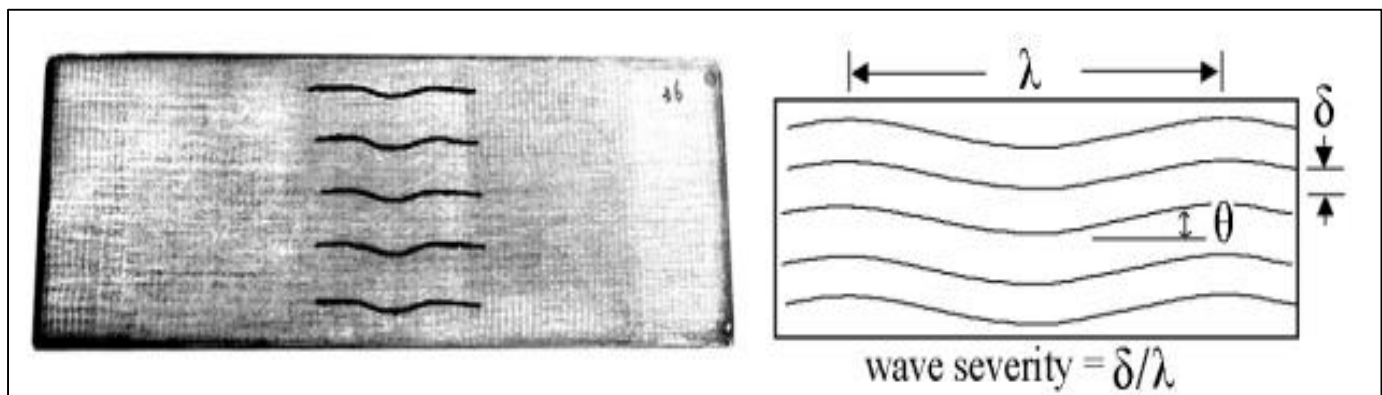


Figure 05: Laminate with Introduced Waviness (left) and Waviness Characterization (Right) [40].

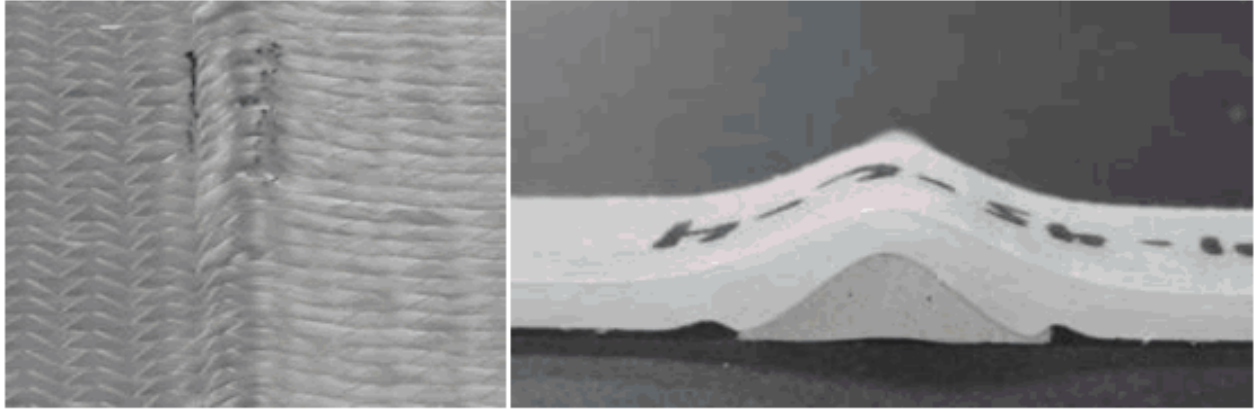


Figure 06: IP waves imparted into a layer in a 0° laminate (left) and an OP wave form used to impart necessary wave into a 0° laminate (right) [41].

Uniform, graded and localized waviness in unidirectional laminates were further studied and explored analytically by Hsiao and Daniel [17] [18]. They also studied the effects of nonlinear waviness under compressive loads [Figure 07]. It was found out that the anisotropy in materials resulted in reduction of strength for a wavy laminates. This result had a good agreement with the analytical predictions made in the beginning. The research also showed that inter laminar shear strengths had a significant influence and was the dominant cause of failure when compared to delamination and buckling of layers under axial compression. It was found that wavy laminates undergo no shear deformations because their effective response tends to remain orthotropic [40].

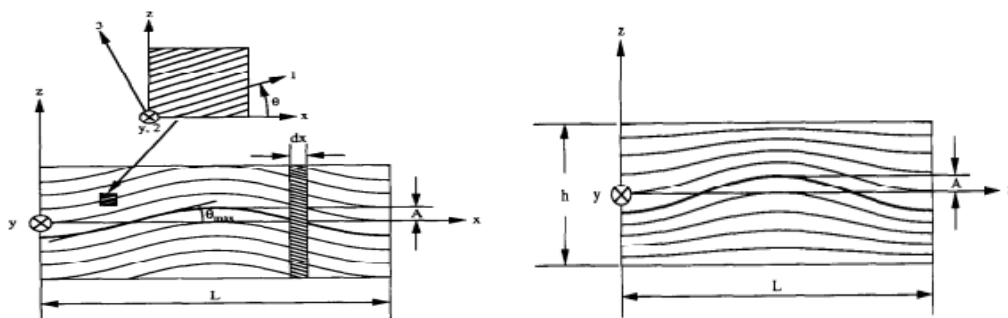


Figure 07: (a) Representative volume and coordinates for a unidirectional composite with uniform waviness. (b) Representative volume and coordinates for a unidirectional composite with graded waviness [17]

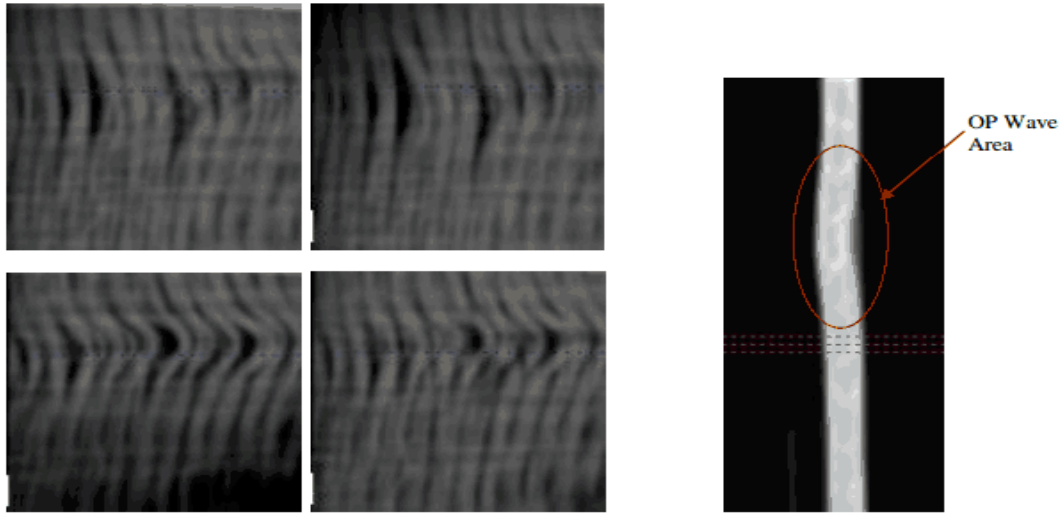


Figure 08: (a) Layer by layer in-plane flaw by radiography. (b) Out of plane defects identification by radiography



Figure 09: (a) Tow thinning seen in a fabric on shifting 35° (b) Out of plane defects identification visual inspection for 25° Shifted fabric.

Wisnom and Atkinson [19] induced waviness artificially in the plies of the laminate by performing the prepreg on a curved plate. In-plane waviness of the fibers was observed on the surface plies along with out of plane waviness in the layers of the laminate. They followed pin ended buckling tests on the laminate coupons to find 17-26% reduction in overall compressive and tensile strains. Thinner portions, where the waviness was seen very evidently had smaller magnitudes in strain. Subsequent to that, Shin and Chun [20] investigated the tensile and compressive response of unidirectional laminates with fiber waviness. The main focus of the

study was to theoretically and experimentally examine the effects of material and geometric nonlinearities on fiber waviness in composite materials. The research was focused on uniform, graded and local fiber waviness patterns commonly found in the laminates. The analytical model showed a reduction in Young's modulus along the longitudinal direction. It was also shown that the degree of fiber waviness influences the strength of the laminate. Also, it was shown that tensile loads cause stiffening of fibers while compressive loads cause softening of the wavy fibers. Fleck and Liu [21] predicted the initiation of micro-buckling in a wavy laminate subjected to compression using a one dimensional infinite band analysis and a failure sample is show in the *figure 10*. They also used the bending theory to predict the compressive strength as a function of amplitude and size of the waviness in the laminate.

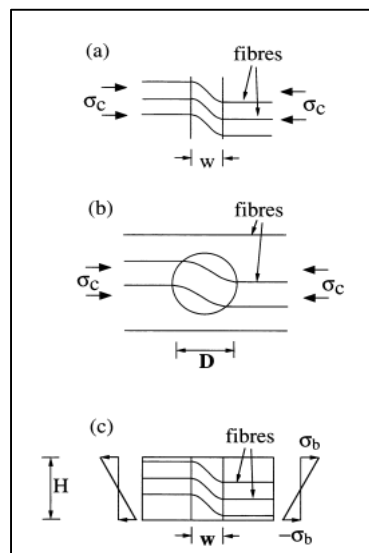


Figure 10: Geometries of imperfection considered in a unidirectional fiber composite: (a) an infinite band of waviness; (b) a circular patch of waviness, and (c) a beam containing a parallel-sided band of waviness under bending [21]

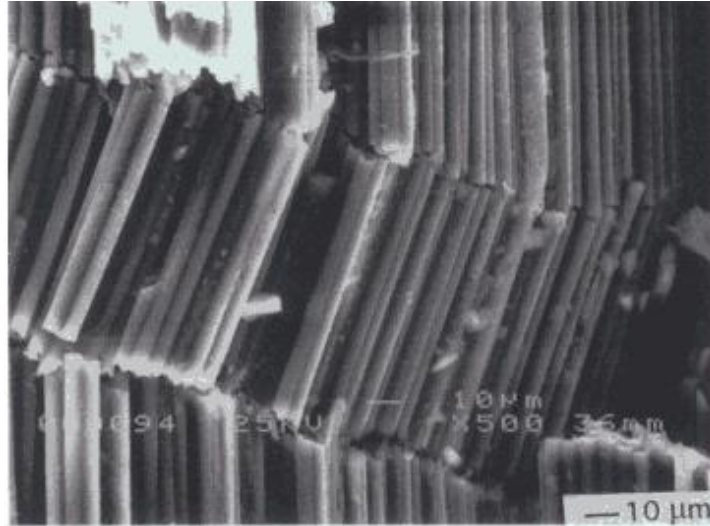


Figure 11: Micro-buckling Failure of a Wavy Composite Laminate Subjected to Compressive Loads [22]

A semi-automated digital imaging technique was developed by N. A Fleck to measure the 2D in-plane distribution of fiber waviness, and the 2D power spectral density function has been determined for random waviness in fiber-epoxy composites. This technique has the important advantage of integrating fiber misalignment information from relatively large regions of the material. There are lots of studies done on the deformation occurring by manipulating the fabric to certain shapes. From the study Robertson [24], it is concluded that Pin Jointed Net (PJN) is the best suited for the studies. The point where the fiberglass from two different directions meets are called joint and any change in the direction from initial position causing the shear affects the joint that causes deformation to the fabric.

Fabric Layup and Resin infusion

One of the major methods adopted for layup is tape layup wherein narrow strips of prepreg are placed in the desired location, shape and fiber orientation within the mold. The prepreg has the adhesive property which makes it stick to the mold and it has the near net shape components with uniform thickness [26]. Vacuum forming is the other process adopted for automated fabric layup. A positive mold is pulled to a negative mold using a vacuum force to

makes the fabric fit. Least resistive shear angle distribution is achieved doing this method because the fabric does not drag on the mold when caught with the vacuum. Due to limitations of the mold geometry shape, it is suitable only for flat, concave and convex shape. Complex parts are not suitable for this process and are not capable of manipulating fiber orientation. Applications of using multiple fabric layup are also limited in this process. This process also has the tendency to make the fiber reach or exceed the shear lock limit [27] [28].

The effect of layer shift on the mechanical behavior of woven fabric laminates has been examined using finite element analysis by Page [42]. Simplified two-dimensional generalized plain strain models have been developed for laminates in which the neighboring layers are in phase (no layer shift), out of phase, or 'staggered' with respect to each other (*Figure 12*). A new method of automation layup was developed by Buckingham and Newell that uses a multi axis robot to place the prepreg material in the mold. Using the foam and air compression, the air inclusions were removed after layup, but the effect of in-plane deformation using these tools were not considered or studied for complex shapes. Following to that, device was made by Shirinzadeh that studies the path of the prepreg layup and based on that it determines the right force to remove the air inclusions based on the feedback [29] [30].

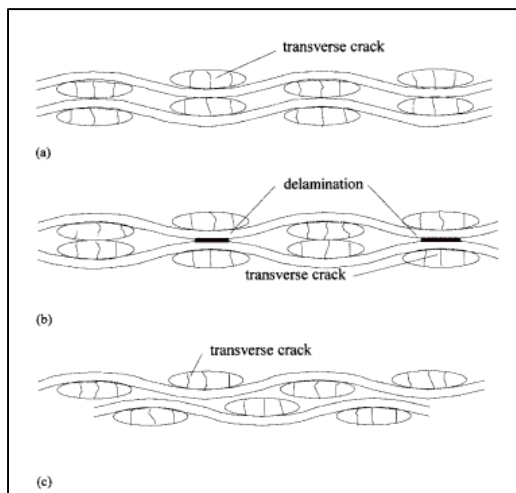


Figure 12: Schematic edge views of damage morphologies in two layer PW GFRP laminates, indicating different relative layer positions: a in phase; b 180° out of phase; and c at some intermediate or staggered phase difference (loading left to right for each figure) [42]

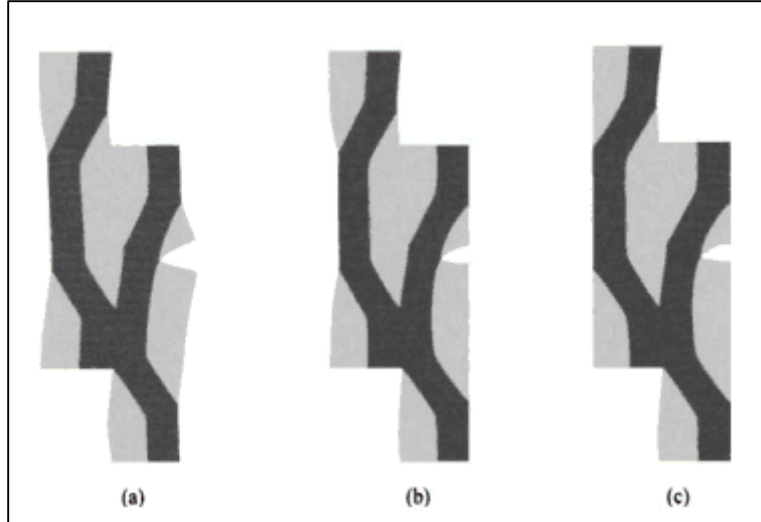


Figure 13: Deformed meshes for staggered geometry with increasing number of layers in model and crack located adjacent to crimp: a two layers; b four layers; c infinitely thick

The time to cure and the temperature at which the resin is cured is important for the properties of the composite materials. One of the factor that affects the resin curing is the tooling material. The tooling method and material also needs to be taken care while shifting followed by infusion. Therefore, the study done by Kantharaju [10], shows how important it is to make an informed choice of tooling materials because of the differential spatial or temporal gradients between the tool and the composite part that are formed during the cure cycle. The low thermal diffusivity of the tooling materials such as steel, brass and copper enhance formation of temperature gradients in the composite material. The effects of these gradients enhance when the temperature during curing reaches the glass transition temperature. Large temperature gradients cause a portion of the laminates to consolidate the transfer of loads while the remaining regions are soft. This effect tends to change the position of laminate layers during consolidation.

Increase in temperature above the glass transition causes a drop in resin viscosity and hence the load required for fiber motion is also reduced. For some matrix materials the viscoelastic behavior is nonlinear even at low strength levels. The free volume inside the matrix and mobility of the polymeric chain cause physical aging. This significantly influences

viscoelastic properties in the matrix. Accelerated cooling is one of the reasons for insufficient relaxation of viscoelastic strength in composite part. This causes fibers to experience elastic deformation leading to waviness in profile.

Compressive testing and failure

Before investigating deep into the effects of shifting that causes in-plane waviness, a review into general compression [Figure 14] and fatigue cycles of composite fabric material is essential. Past studies of fiberglass laminates have reported that compressive strengths and failure strains which are suitable for wind turbine blade designs are depending upon the reinforcement architecture, matrix resin, and environment. Compressive strength is known to be sensitive to the straightness of the fibers, with even relatively small degrees of waviness or misalignment causing significant decreases in compression properties [4]. The distribution of compressive strength has been predicted using a finite element program, which includes the effect of fiber misalignment and the relative length scale of the waviness to the fiber diameter. It is found that the predicted, and measured, spread in compressive strength can be represented by a Weibull distribution. Thus, a methodology has been developed to predict the statistical distribution of compressive strength from the measured random waviness pattern [9]. The properties of the fibers, matrix and the interface of fiber-matrix regions in the laminate affects the compressive strength. The focus of the investigations has been to carry out analytical modeling and conducting experimental tests.

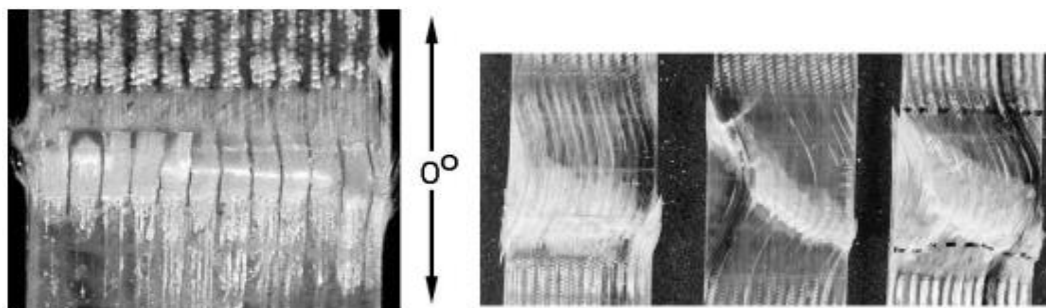


Figure 14: (a) Static Compression Failure Mode for a Typical Unidirectional Fabric for the 0° Plies, (b) Compression Failures for Glass Fiber Laminates Containing Induced In-Plane Waviness [40]

There are lots of analytical models created by researchers to predict and estimate the effects of waviness on strength and stiffness of laminates when subjected to compressive force. A major investigation was done by Rosen [11] on the prediction of compressive strength of straight fibers based on micro-buckling model. The study predicted the strength based on kinking of fibers [Figure 15] under buckling condition and came up with equation: $\sigma_c = \frac{G_m}{(1-v_f)}$ where G_m is the matrix of shear modulus and v_f is the volume concentration of fibers.

Later on, when Fleck and Bundiansky [12] investigated the same problem, they found that Rosen prediction of compressive strength of composite materials was over predicted. They found that the strength around the kink-band was one fourth less than the composite materials with straight fabric. From various research investigations, it was found that the compressive strength for a composite laminate is only about 60% of its tensile strength. Studies on compressive tests becomes complex due to the buckling effect or due to the inter-laminar shear failure, matrix cracking splitting which lends the matrix incapable of supporting the fibers, inducing failure in the laminate. Consequently, under the action of compression loads, the resin rich areas experience a reduction in the in plane load carrying capability inducing matrix dominated failure modes in the laminate [10].

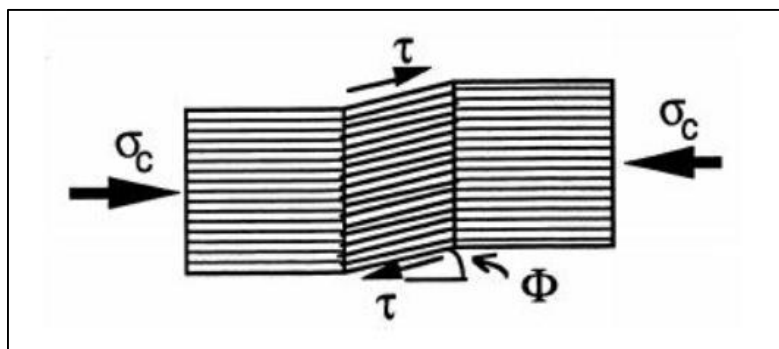


Figure 15: Alignment of Kink Band with respect to Longitudinal Axis [12]

Fatigue cycle testing and failure

Fatigue is the condition whereby a material cracks or fails as a result of repeated (cyclic) strengthes applied below the ultimate strength of the material. The phenomenon of fatigue

which has been estimated to be responsible for up to 90% of the in-service part failures which occur in industry. Fatigue failure can be understood as a loss of adequate stiffness or adequate strength. There are two approaches to determine fatigue life; constant strength cycling until loss of strength, and constant amplitude cycling until loss of stiffness. The approach to utilize depends on the design requirements for the laminate. Frequency is one of the critical parameters in fatigue testing. Frequency is highly related to the life of the test, hence higher the frequency, lower the fatigue life is. Extensive testings have been done at Montana State University with varying frequency and loads. Most of other time, fatigue life had higher impact from frequency [34].

Fatigue behavior of composite materials and structures is a phenomenon consisting of cyclic thermal or mechanical load-induced events and processes over time which determines long-term performance. These events, generically called damage in the composites literature [14], combine in such a way as to change the response of the composite to the extent that it may fail to satisfy its intended service requirements. The strength of a material over its lifetime is commonly understood by doing the fatigue testing. Loading of laminates for fatigue testing is important and can influence the fatigue life. Composite materials showcase very complex failure mechanisms under static and fatigue loading because of anisotropic strength and stiffness behavior. The complex failure mechanisms involved depends on many parameters such as fiber and matrix materials, geometry, load levels and, stacking sequence. Most of the structural components are subjected to continuous loading and unloading and hence this fatigue life study is very critical. Factors like fiber orientations, loading sequence and materials makes the fabric highly complex in terms of studies and properties. Since these materials are used for various purpose, the failure points are determined based on its applications.

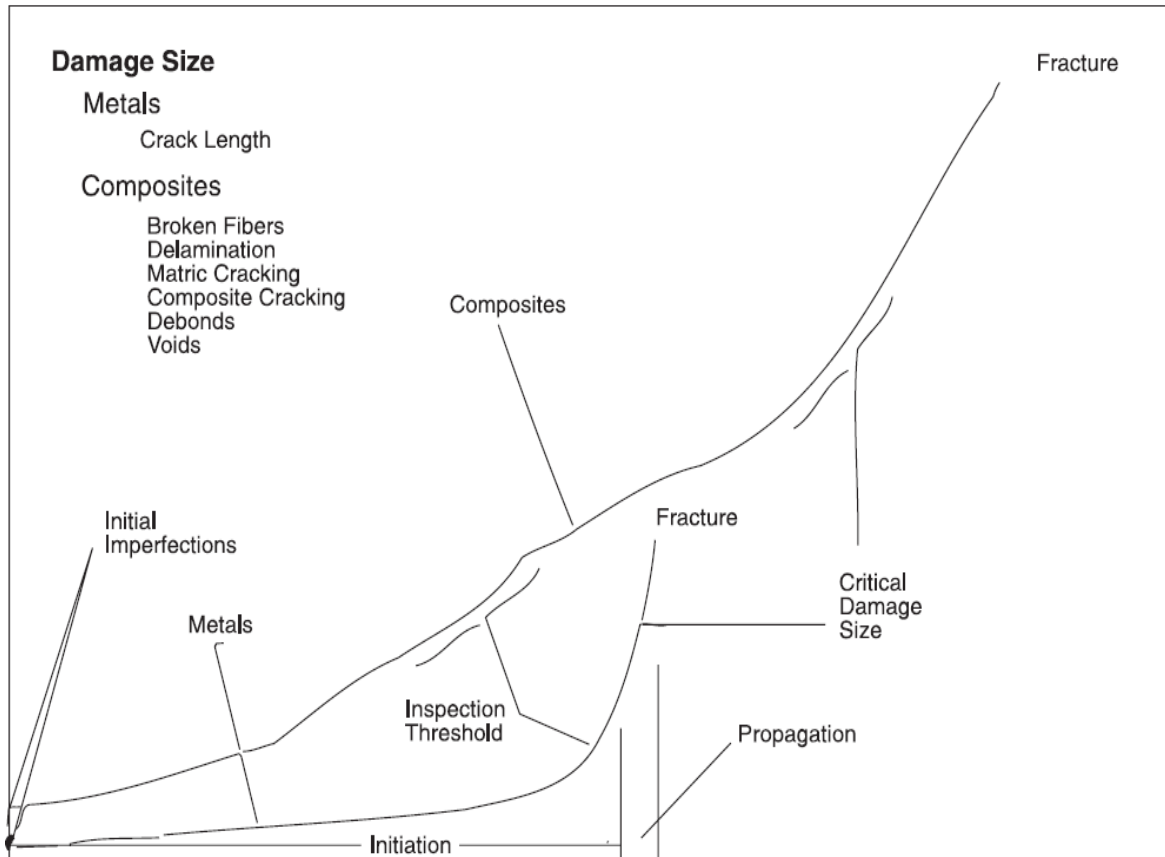


Figure 16: Typical Comparison of Metal and Composite Fatigue Damage [Salkind, Fatigue of Composites]

Wahl and Samborsky [35] studied different spectrums of loading conditions on composite materials. Coupons were used for the tests with same strength level loadings but varying load values. It has been found that varying loads did not have much impact on the fatigue life of the composite coupons. The edges on the coupons are prone to faster cracking as the strength concentration is high at the edges due to change in fiberglass orientation. The edge splitting phenomena due matrix orientation while fatigue testing or compression testing is also shown by Mandell due to strength concentration (*Figure 17*). Fiber orientation, in-plane waves and out of plane waves were taken into consideration while studying the fatigue life of the composite coupons. Finally, amplitude and wavelength comes into light while characterizing the material properties of composite.

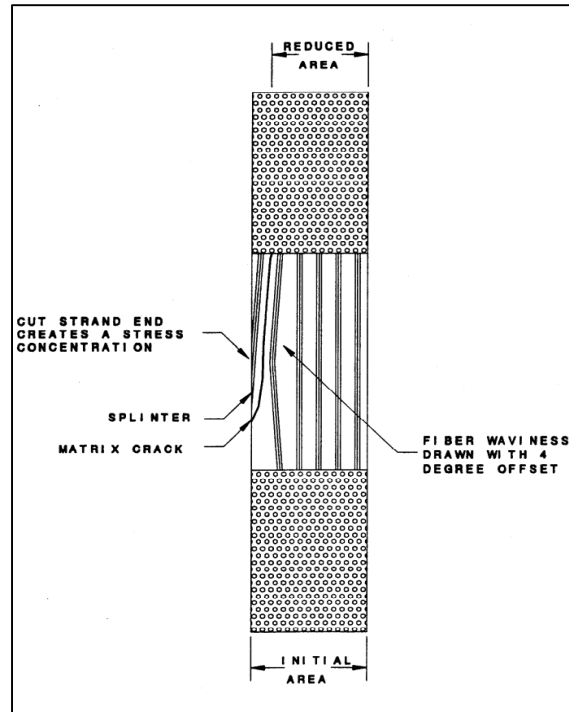


Figure 17: Schematic of Edge Splitting in Unidirectional Materials [35]

The Fatigue Life (N_f) of a component is defined by the total number of strength cycles required to cause failure. Fatigue Life can be separated into three stages where $N_f = N_i + N_p$

- 1.) *Crack Initiation (N_i)* - Cycles required to initiate a crack. Generally results from dislocation pile-ups and/or imperfections such as surface scratches, voids, etc.
- 2.) *Crack Growth (N_p)* - Cycles required to grow the crack in a stable manner to a critical size. They are generally controlled by strength level, since most common materials contain flaws; the prediction of crack growth is the most studied aspect of fatigue.
- 3.) *Rapid Fracture* - Very rapid critical crack growth occurs when the crack length reaches a critical value and this happens very quickly and is difficult to term it.

In a unidirectional fiber composite, cracks may occur along the fiber axis, which usually involves matrix cracking. Cracks may also form transverse to the fiber direction, which usually indicates fiber breakage and matrix failure. The accumulation of cracks transverse to fiber direction leads to a reduction of load carrying capacity of the laminate and with further fatigue

cycling may lead to irregular failure of the composite material. Hahn [38] predicted that cracks in composite materials propagate in four distinct modes. These modes are illustrated in *figure 18*, where *region I* corresponds to the fiber and *region II* corresponds to the matrix. A detailed analysis of the progression of fatigue damage in laminates is shown in *figure 19*. This analysis considers tensile, compressive loads and a variety of laminate ply orientations [43].

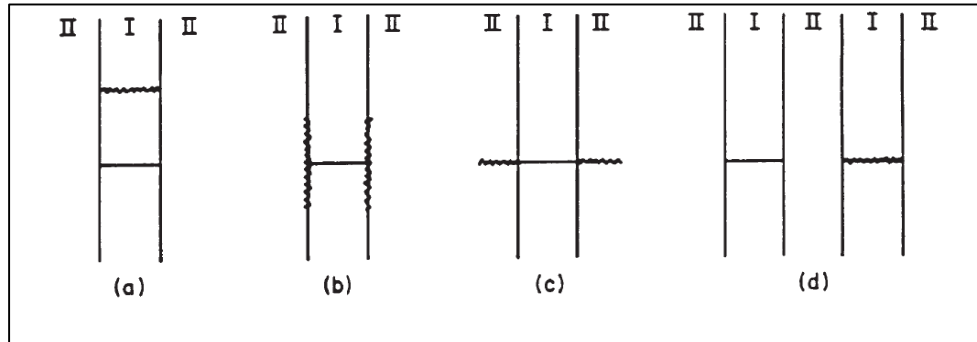


Figure 18: Fatigue Failure Modes for Composite Materials - Mode (a) represents a tough matrix where the crack is forced to propagate through the fiber. Mode (b) occurs when the fiber/matrix interface is weak. This is, in effect, de-bonding. Mode (c) results when the matrix is weak and has relatively little toughness. Finally, Mode (d) occurs with a strong fiber/matrix interface and a tough matrix. Here, the strength concentration is large enough to cause a crack to form in a neighboring fiber without cracking of the matrix. Mode (b) is not desirable because the laminate acts like a dry fiber bundle and the potential strength of the fibers is not realized. Mode (c) is also undesirable because it is similar to crack propagation in brittle materials. The optimum strength is realized in Mode (a), as the fiber strengths are fully utilized. [38]

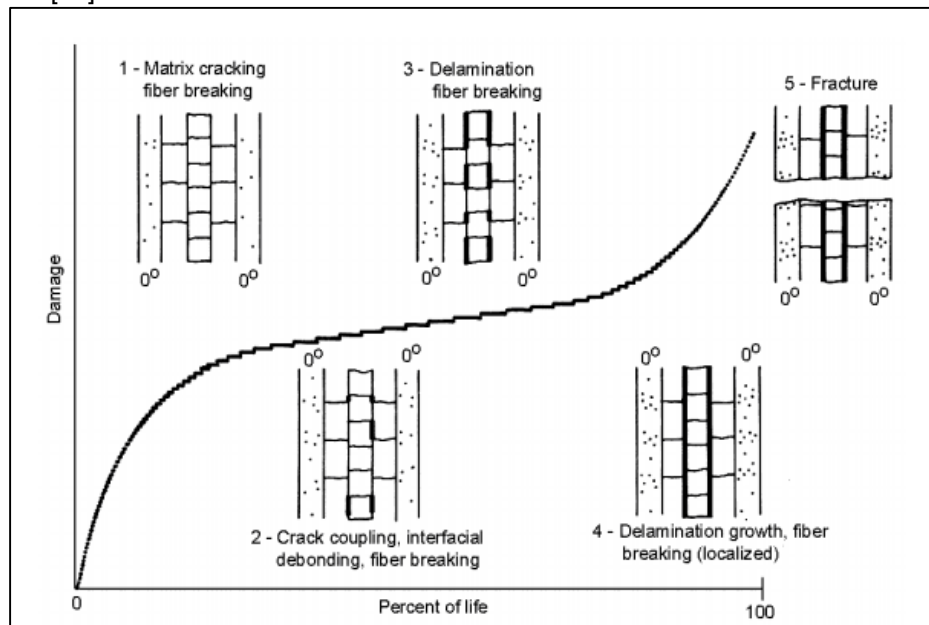


Figure 19: Schematic representation of the development of damage during the fatigue life of a composite laminate [43].

Chapter 3: Research Goals

The feasibility of the shifting machine, its impact on the fabric and how it affects the normal life of the composites was discussed in this research. The study investigated the deviation from the expected properties of the composite materials from shifting.

1. What is the impact of the fabric shifting on the composite material properties?
2. What is the acceptable shift angle for the fabric for which it can be assumed to be safe for practical applications?
3. Is it only the shifting that is causing the change in properties or is there any other potential reasons causing the change in mechanical properties of the composites?

Chapter 4: Methodology

The methodology will include finding the shear lock limit of the fabric, followed by sample preparations and setting up of the test stands for the experiments. Determining the compressive and fatigue properties of the composite samples from the experimental tests will be discussed. A similar life cycle replications of actual applications are done to test the qualities of the parts made out of these shifted fabric. The samples made out of the shifting machine are subjected to fatigue cycles. Here compressive-fatigue is preferred over tension fatigue which prevents the fiberglass and cross-tow from breaking in the initial stages of tests.

Shear-lock limit

The shear lock limit (*figure 20*) is the maximum extent to which the fabric can be shifted without any out of plane waviness or breakage of the linkage. The manual shear locking limit measuring equipment used in this study is shown in *figure 21*. A single ply of fabric was clamped in the manual shifting machine with a distance of 40 cm between the two clamps. This manual shifting mechanism is a setup with four armed rectangle shape seen in *figure 21*. A fabric is clamped on two of the opposite arm and a rotating mechanism which transform the rectangular shape to parallelogram thus creating a shift in the fabric. This machine is referred to as manual shifting machine.

A perpendicular line was drawn on the fabric to the direction of the fiberglass to visually analyze the fabric deformation on shifting. As the machine transforms in shape by rotating the knob, the fabric clamped to it also takes that shape creating tension in fabric. The fabric was shifted until the fabric started showing signs of out-of-plane waviness. The out-of-plane waviness were characterized by the fabric when the fabric loses the flatness by any sorts of deformation especially wrinkling. The extent of shearing a stitched non-crimp fabric until the shear locking limit is surpassed and out-of-plane deformations are produced is called the shear

lock limit. As shearing approaches the locking limit, the tow spacing and width of tow and entire fabric is reduced [44]. The shear lock limit for the unidirectional fabric was found to be 41 degrees, but at this high shift angles, the clamping points were weakened due to the breakage of cross tows and thinning of tows. The tows thinning results in change of fabric geometry when the fiberglass within the tow overlap each other reducing the width of tows, but increasing the thickness. Right after shifting a fabric to a certain angles, the fabric straightens back nearly 21.8% back. This value is experimentally found by measuring the theoretical shift angle and actual angle of shift in the fabric [Table 2]. This phenomenon of straightening the fabric after shifting is referred as spring-back in this study.

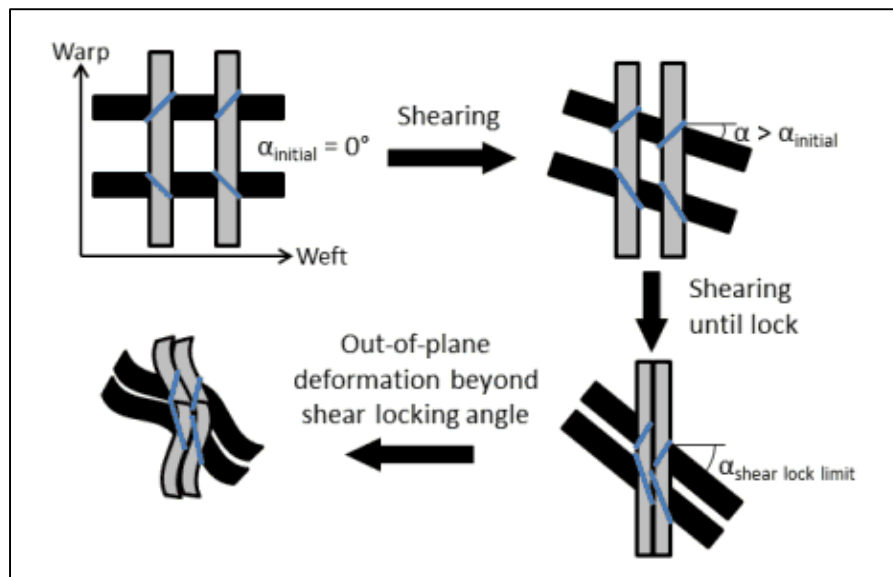


Figure 20: Schematic representation of the shear lock limit within fabric tows [44]



Figure 21: [a] Shear lock limit testing setup; [b] The shear lock limit measuring on an unidirectional fabric

Experimental design

The shifting machine is made of joined aluminum frame to create a hollow box frame seen in figure 22. The unidirectional NCF fabric are in the form of 200 mm roll which is attached to the top of the shifting machine roller mechanism frame which unwinds as the machine shifts. The fabrics from the roll is passed through front and back pinch roller which helps to pull the fabric from the fabric roll. There is a shifting clamp and a spacing clamp between the pinch rollers. The spacing clamp moves in x axis based on the shift input while the shifting clamp moves in y axis which creates the shift to the fabric. The shifting clamps and pinch rollers are opened and closed pneumatically. This whole aluminum frame is hanged on the motor and chain mechanism which is capable of moving in x, y and z axis. Unidirectional NCF fabric was used throughout this research.

The fabric shifting machine shifts the fabric according to the user input and lays it on the table which is kept below the shifting machine. In my study, each layer of fabric was shifted only once, hence after each shift, the fabric is laid on the table. The fabric is cut out from the end of the roller after each shift. The machine is then brought back to the initial position where the machine was previous to the first shift to ensure the next layer of fabric are laid by overlapping the shift location without any offset. This process is repeated 4 times to get four layer of shifted fabric which is considered to be a sample.

Prior to making samples, 6 unidirectional NCF fabrics were shifted to various angles starting from 0 to 25 at an increment of 5 degrees each time. The actual angles of these fabrics were measured against the applied shift angles and tabulated in table 2 to determine the spring back. The actual angles were measure using a digital protractor and it was noticed that there is an average *spring back* of 21.8% to the fabric after shifting. The stack of fabric layers are then carefully moved to an infusion table for resin infusion.

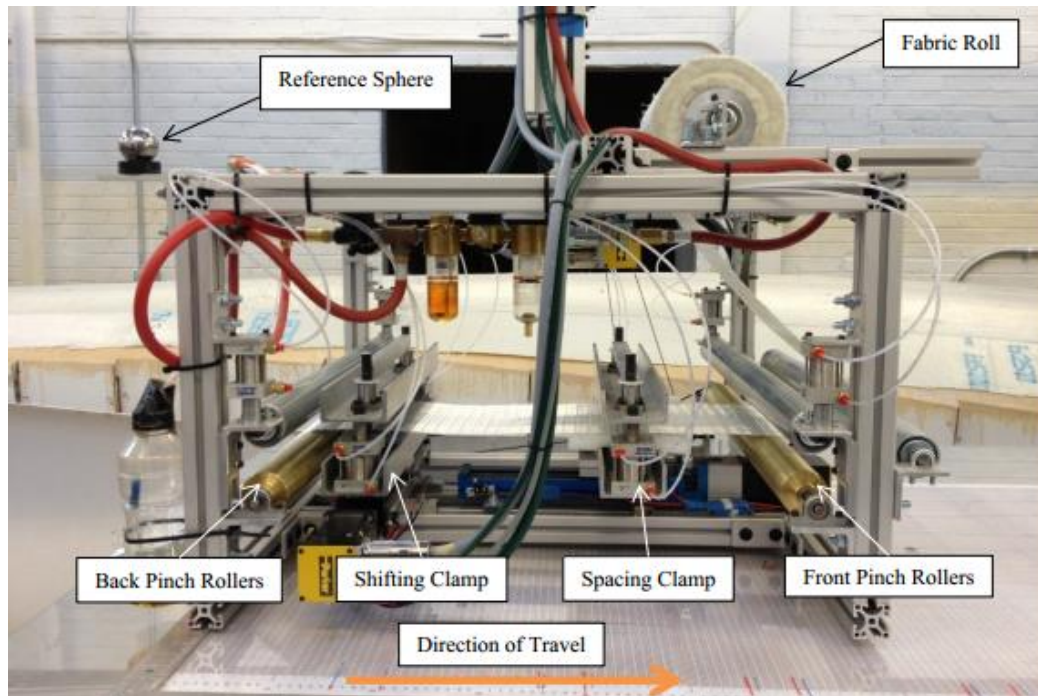


Figure 22: The fabric Shifting Machine at Iowa State University [Siq].
The samples were infused using resin transfer mold method as seen in the figure 23.

The infusion bag, peel ply, breather is all cut into desired shape and size to create the setup for infusion. Hexicon EPICURE™ resin MGS RIMR 135 and EPIKURE™ Curing Agent MGS RIMR 1366 were mixed in the ratio 1:3 by weight. This mixture is blended together and placed in vacuum jar to release all trapped air bubbles. The infusion process is left until the resin solidifies and stops the further flow. The samples after resin infusion were let to cure for 24 hours under the heat lamp to avoid the varying temperature influencing the curing time.

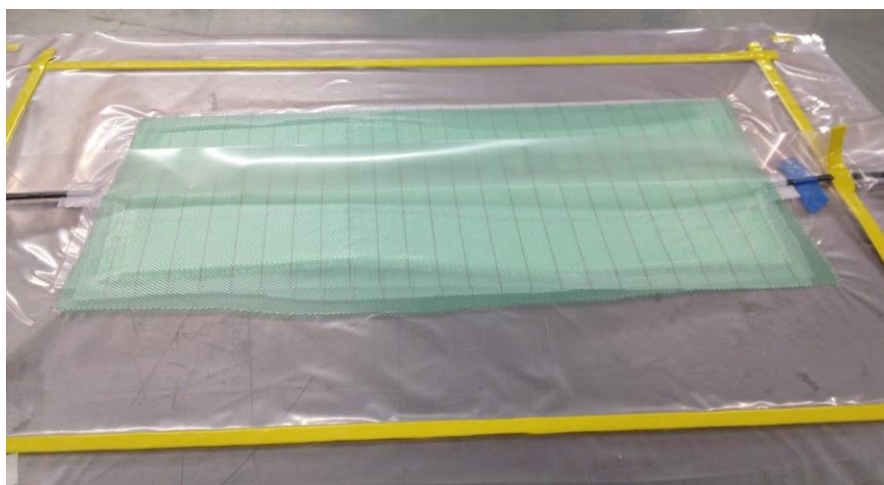


Figure 23: Resin infusion process to create the 4 layered sample.

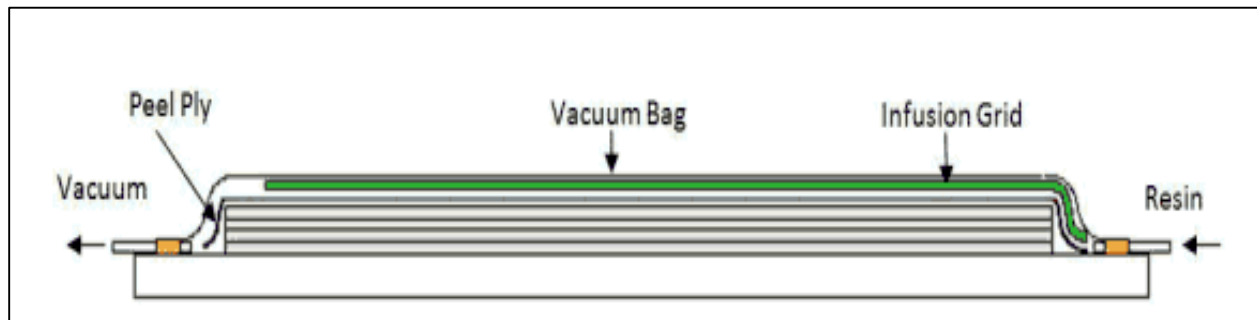


Figure 24: Cross sectional view of the resin infusion setup [39]

Test setup- making of coupons, geometry, equipment used

The coupon geometry is very critical in the fatigue tests and compressive tests. Samples were made based on the ASTM standards [ASTM D3410/D3410M]. This is a standard test method for compressive properties and sample preparation of polymer matrix composite materials. According to this standard, the test specimen shall have a constant rectangular cross section with a specimen width variation of no more than $\pm 1\%$ and a specimen thickness variation of no more than $\pm 2\%$. It also emphasizes that both the specimen width and thickness shall contain a sufficient number of fibers. The coupon geometry requirements are given in table 3 of appendix A. A water cooled power tile saw *IMER Combi 350-1000* with a 35 cm diameter diamond coated blade rotating at 2190 rpm was used to cut the coupons out of the sample. Samples with 0 degree (straight sample) followed by 5, 10, 15, 20 and 25 degrees were made and from each sample, 6 shifted and 2 straight coupons of 130 mm long and 25 mm wide coupons were cut. A gap of 3 cm was left while cutting out the shifted coupons [Figure 25]. The feed rate of the sample for cutting was 5mm/sec to ensure a clean cut. This high rpm and lower feed rate minimizes notches, undercuts, rough or uneven surfaces and delamination. The edges of the samples were polished with sandpaper (Grit 600) to smoothen the edges. *Figure 25* explains the coupons cut location from a sample.

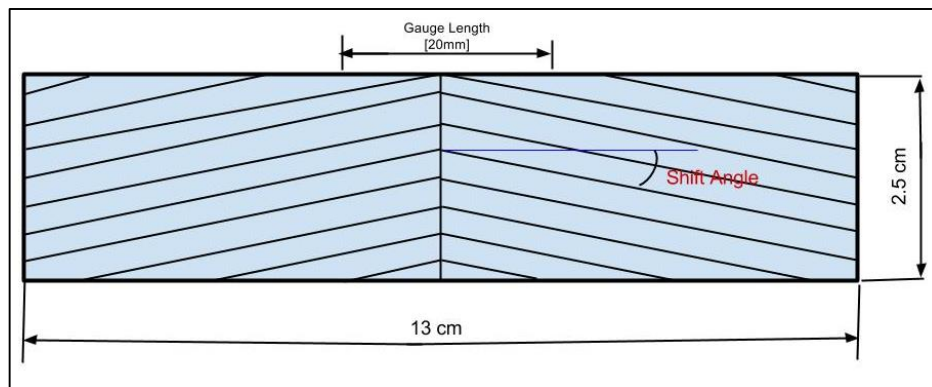
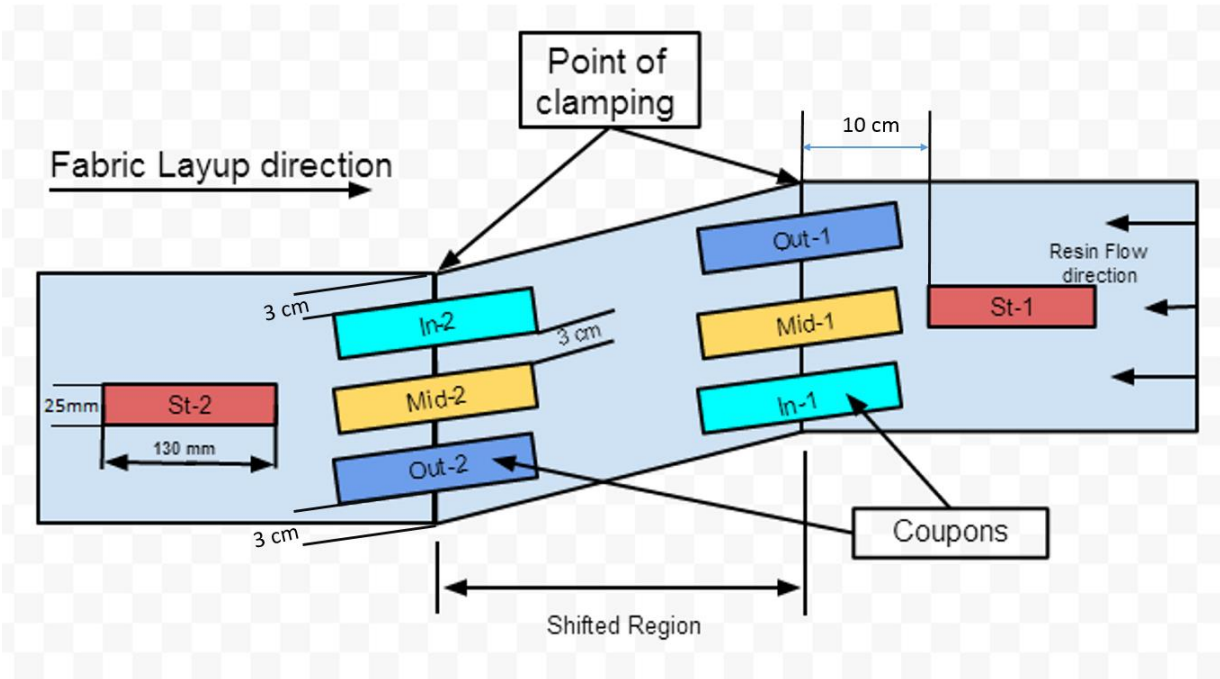


Figure 25: (a) Diagrammatic representation of the sample after infusions and the coupon location (b) Coupon structure and orientation

Compressive Tests and Compressive-Fatigue Tests

Flat coupon having a constant rectangular cross section is loaded in the compression tester Instron 8801 [Figure 27] by shear force acting along the grips to obtain the ultimate compressive strength values. Two shifted coupons per samples were tested for compressive tests and two samples for fatigues tests. Each of the tests were replicated with the same parameters. The testing machine with a double acting servo-hydraulic actuator has a force

capacity up to $\pm 100\text{kN}$. The sideways moment of the base actuator was resolved by placing a small rod and a guiding clamp connected to the machine frame on one side of the actuator. This procedure eliminates torsional rotation of the sample during compression and fatigue tests. The compressive force is applied via the wedge holder shown in the *figure 28*.



Figure 26: (a) Instron 8801 compression and fatigue testing machine used in the study (b) Instron 3580 Hydraulic power unit

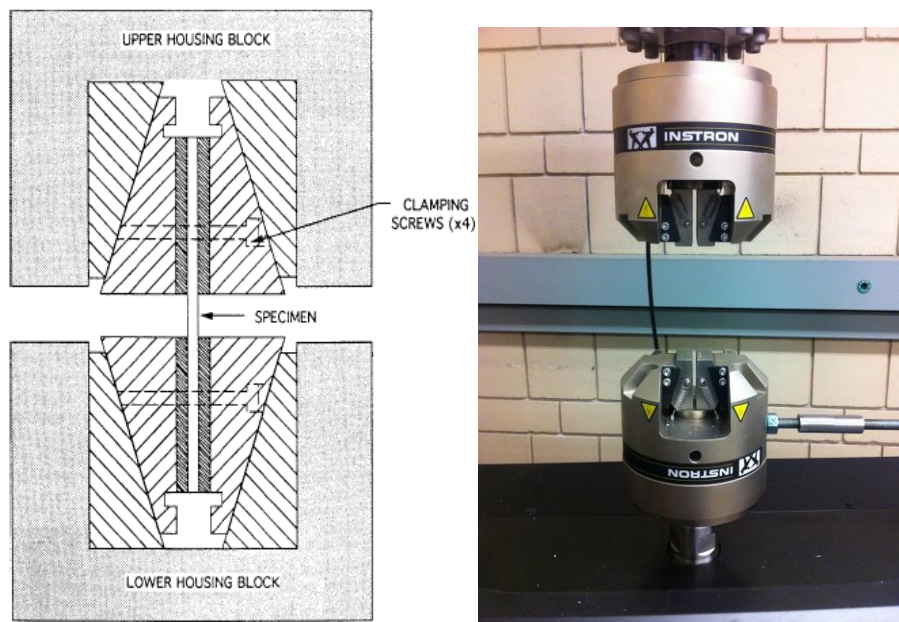


Figure 27: (a) Schematic of Compression Test Fixture [45], (b) Actual jaw and head of the testing machine

Compression tests for any materials are difficult due to premature failures or the buckling of the samples which result in undesired results. The specimen length, width and thickness were given as input in the Wavematrix software for the output of compressive load, strength, strain and yield. The ultimate strength is obtained from the maximum force carried before failure of the coupon. Strain is monitored with displacement transducers so the strength-strain response of the material can be determined, from which the ultimate compressive strain, the compressive modulus of elasticity, Poisson's ratio in compression, and transition strain can be derived.

Since compressive and fatigue tests are sensitive to the alignment of the specimen in the fixture, coupons are marked prior to the tests. These markings are aligned with the wedge edge to prevent any misalignment of specimen. The gauge length has to be short enough to avoid any Euler buckling, yet long enough to allow strength decay to uniaxial compression and to minimize Poisson restraint effects as a result of the grips. The recommended specimen gage length is 12 to 25 mm [0.5 to 1.0 in.] to balance the competing requirements of strength decay length and Euler buckling length [45]. The specification followed in ASTM D3410 limits the amount of buckling and helps in obtaining representative compressive properties. There is a high probability for tabs induced failure in these composite materials and hence tabs are not used in these coupons.

The gripping surface is rubbed and roughened with sandpaper [Grit 100] to avoid slippage while in compression. Compressive strength for the same materials has shown different values at different trials. Such differences can be attributed to specimen alignment effects, specimen geometry effects, and fixture effects even though maximum efforts have been made to reduce these effects. Flatness and parallelism of the coupon are sensitive to the result and hence extreme care has been taken care while loading the specimen. The upper wedge housing block assembly is attached to the upper crosshead of the test machine while the lower wedge housing block assembly rests on a lower platen. Force is transmitted to the specimen via

a tapered wedge grip. One of the grips is constant and the other grip head is compressed with the desired speed [.05in/min] until the specimen cracks or breaks. The failures are identified based on Three-Part Failure Identification Codes standard criteria shown in *figure 30*.

Compression tests were performed with the coupons with varying shift angle to determine the ultimate breaking force. These forces were kept as the reference to run the fatigue testing. The R value which is the ratio between minimum cycle strengths to maximum cycle strength was kept as 0 because compressive fatigue testing was used. Keeping the R value 0 for the fatigue test prevents any extension of fabric. For testing efficiency, the coupons were fatigue tested at 85% of the ultimate compressive load at a frequency of 5 Hz. When there were no signs of failure on the coupons after 130 thousand fatigue cycle, the coupons were then run at 90% of the load.

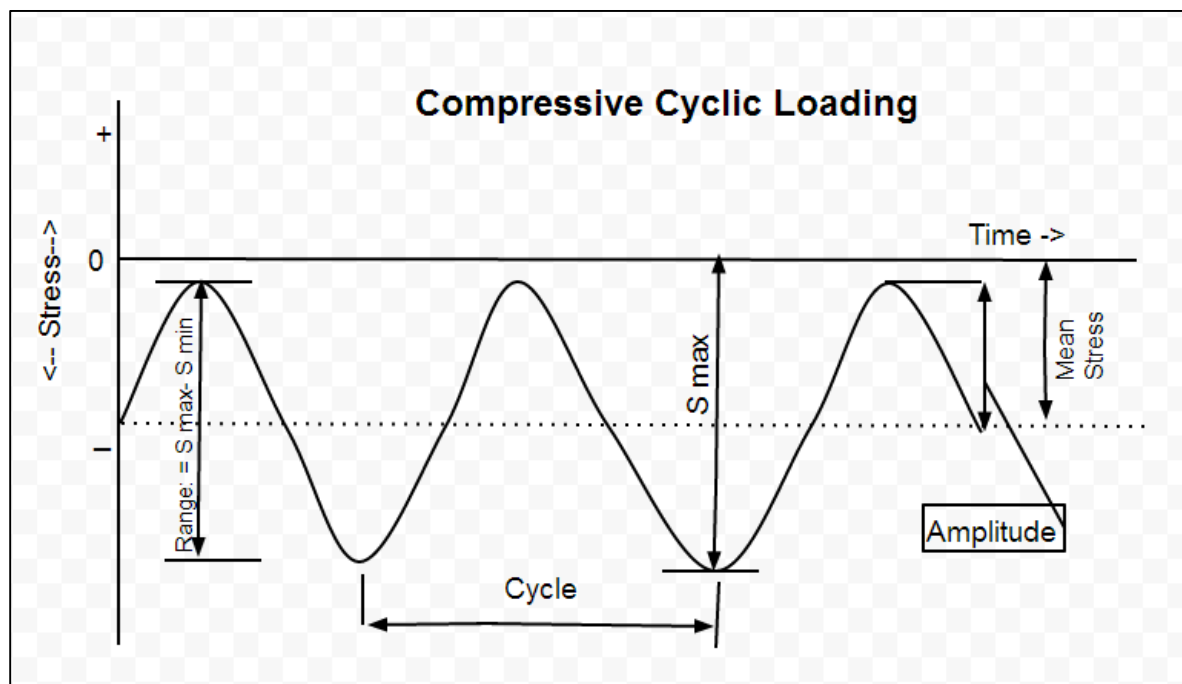


Figure 28: Schematic Illustrating Compressive Cyclic Loading

The following parameters are utilized to identify fluctuating strength cycles:

Mean Strength (σ_m):
$$\sigma_m = \frac{S_{\max} + S_{\min}}{2}$$

Strength Ratio (R) :

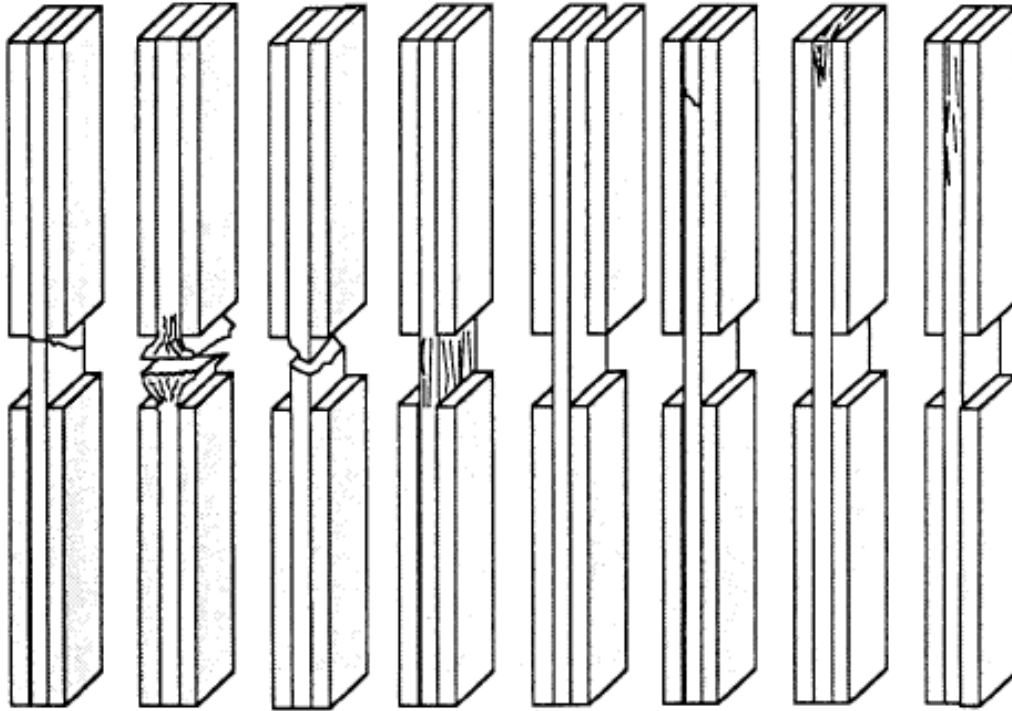
$$R = \frac{S_{min}}{S_{max}}$$

Strength Amplitude (σ_a) :

$$\sigma_a = \frac{S_{max} - S_{min}}{2}$$

Strength Range (σ_r):

$$\sigma_r = \sigma_{max} - \sigma_{min}$$



TAT BGM HAT SGV
Acceptable Failure Modes and Areas

DTT HIT CIT DIT
Unacceptable Failure Modes and Areas

First Character	
Failure Mode	Code
Angled	A
Brooming	B
end-Crushing	C
Delamination	D
Euler buckling	E
through-thickness	H
Kink bands	K
Lateral	L
Multi-mode	M(xyz)
long-Splitting	S
Transverse shear	T
eXplosive	X
Other	O

Second Character	
Failure Area	Code
Inside grip/tab	I
At grip/tab	A
Gage	G
Multiple Areas	M
Tab adhesive	T
Various	V
Unknown	U

Third Character	
Failure Location	Code
Bottom	B
Top	T
Left	L
Right	R
Middle	M
Various	V
Unknown	U

Figure 29: Compression Test Specimen Three-Part Failure Identification Codes and Overall Specimen Failure Schematics [45]

Chapter 5: Results and Discussions

The impact on the properties of the fabric on shifting was analyzed in this study. To compare the effects, the fabrics were shifted at varying angles to create samples and then coupons were cut out of it. These coupons with varying shift angles were subjected to compression and compressive-fatigues tests.

To obtain the results, the fabrics were initially tested to find the shear-lock limit. The shear lock limit from the experiment conducted was found to be 41 degrees for the unidirectional NCF. In conventional fabric layup for wind turbine manufacturing, the fabrics are not shifted more than 8 degree which is 20% of the fabric shift without breaking any tows or fiberglass. During the experiment to find the shear-lock limit, the tow thinning for large shift angles were very evident from visual inspection and can be seen in the *figure 09*. Tow thinning results in bringing the bunch of fiberglass together leaving a gap between tows. The reason for the deformations occurring in the point of clamping location is due to varying radius of curvature within a fiberglass tow [*Figure 31*]. This varying radius of curvature is localized to the location of clamping. The shifting also results in breaking of cross tows and built strength concentration at the point of clamping due to in-plane waviness.

These tow thinnings cause the tows to have higher fiberglass density in the clamping region causing thickness variation and thus creating strength concentrations. The change in fiber orientation by shifting creates in-plane waviness for the fabric. Four of these fabric layers are stacked over each other to create a sample. When layers of in-plane waviness and tow separated fabric are stacked over each other will result in out-of-plane enough to create a clearance when kept on a flat surface. Both in-pane waviness in the fabric ply and out-of-plane waviness for the overall sample created resistance to resin flow during infusion. It took 8-10% more time for the resin to cross the shifted region. The out-of-plane waviness severity was

directly proportional to the shift angle. For the smaller shift angles 0, 5 and 10 degrees, the out-of-plane deformation was little to none.

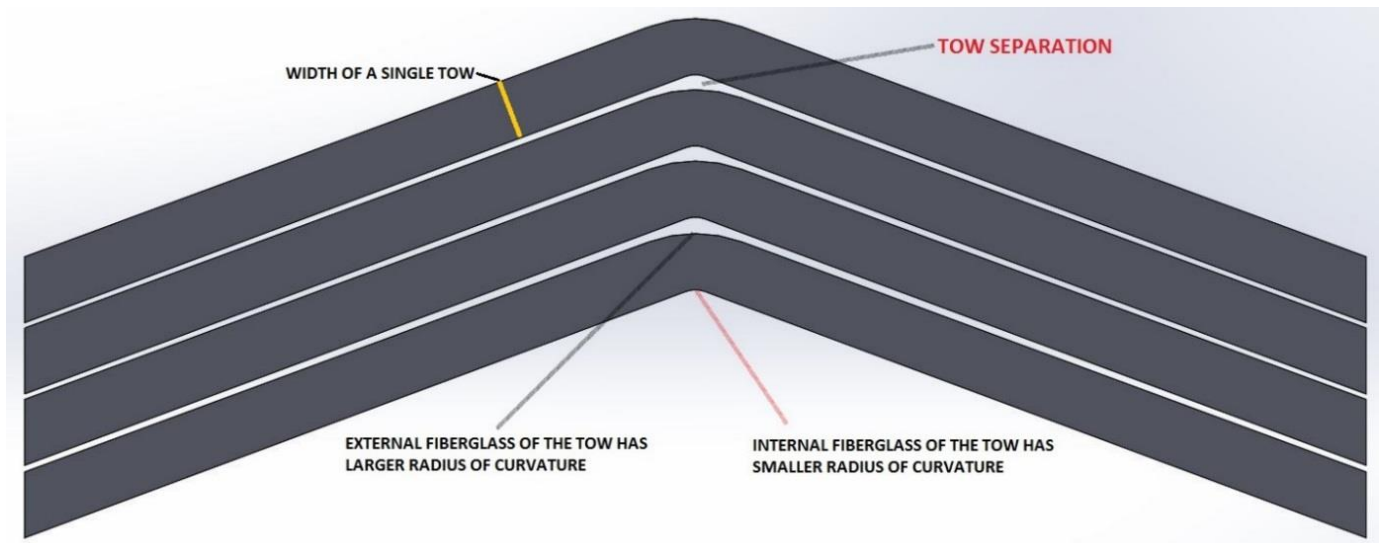


Figure 30: Schematic representation of tow thinning due to varying radius of curvature within bunch of fiberglass in a tow.

Compression and fatigue testing was one of the criteria to determine the properties of the shifted fabric. Two samples per shift angles were used for compression test and two for fatigue tests. The compression tests were differentiated into straight and shifted coupons samples. Six shifted coupons were cut from a single sample, ie 2 from the inside edge, 2 from the middle and 2 from the outside edge coupons. The coupon locations are marked in the *figure 25*. The thickness variation of coupons with varying shift angles varies from .23 - .30 cm and is given in the *table 01*. Two straight coupons were cut from each sample, one closer to the resin entering area and one closer to resin exit area. The purpose of the straight coupons cut out of shifted samples were to provide a baseline if there is any change in properties between straight and shifted fabric within the same sample.

The longest, yet the thinnest rectangular sides of the coupons cutout are sharper and rougher because the fiberglass which are exposed in that surface due to the fiber orientation shown in the *figure 33*. The rough surface can be easily polished using sandpaper [500 grit] for

coupons with 0, 5 and 10 degree shifts. Coupons with shift angles above 10 degree cannot obtain a very well-polished surface using sandpapers due to more fiberglass being exposed.

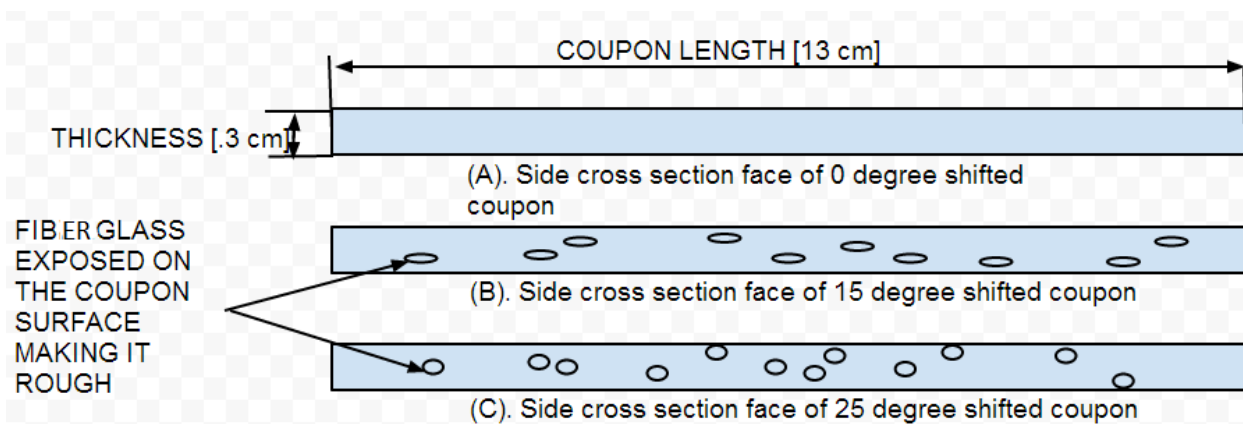


Figure 31: Schematic representation of the side of coupon depicting the cause of roughness due to fiber orientation after shifting.

The samples were all cut into same dimensions, but number of complete tows within the samples varied depending shift angles. For both the compressive and fatigue tests, the samples were clamped such a way that the force acted perpendicular to the fiberglass direction. The ASTM D3410 standard specifies a gauge length between 12 mm and 25 mm to minimize the chance of buckling; a gauge length of 20 mm was used. This gauge length was in the center of the samples where half of the fiberglass direction was mirror image of the other half. This was the same region where the fabrics were clamped for shifting and the maximum number of complete tow passing region. The load carrying capacity and the strength of the coupons depend on total number of complete continuous tows present within those samples. The load carrying capacity of the coupons is inversely proportional to the shift angle due to decreasing in number of continuous tows in coupons. This load carrying capacity in turn is directly proportional to the compressive and fatigue loadings.

The fatigue tests were characterized by compressive loadings without any tensile load and hence both the compressive test and fatigue tests will have similar influence from number of continuous tows present in the coupons. It was found that coupons with 0, 5 and 10 degree

shifts had higher compressive strength compared to higher shifted coupons of 15, 20 and 25 degrees [Table 01]. This was due to the fact that these coupons had relatively more number of complete continuous tows compared to coupons that were shifted above 10 degrees. The set of experimental data collected indicate however that the induced shift angles up to 10 degrees have a very small influence on the strength of this composite. The non-shifted coupons had 7 continuous tows whereas 5 and 10 degree shifted coupons had 6 continuous complete tows which confirms that there was no much strength loss. The ultimate breaking force for non-shifted coupon which carried 7 tows had a compressive strength of 414 MPa which tells us that each tows had a load strength withstand capacity of 59.14 MPa. Similarly for coupons with 5-25 degree shift angles, strength carrying capacity of each tow was 70.16, 65.5, 65.6, 57.4 and 63 MPa respectively which gives an average of 63.46 MPa per tow. When the tows have strength carrying capacity, it is evident that shifting causing reduction in number of tows will influence the mechanical properties of the coupons.

A summary of fatigue tests is given in the table 3 and figure 38 and 39. The ultimate breaking force and compressive strength is plotted against shift angle to underline the trend of shifted samples with varying number of tows influence the mechanical properties. Coupons with 0 and 5 degree shift angles on fatigue tests with 85% breaking force did not fail or showed any sign of failure for 136718 and 230725 cycles. These coupons were then subjected to 90% of the ultimate breaking force in order to fail. We saw the strength carrying load for each tows within a sample for compressive tests with less variation with a standard deviation of 4.67 MPa. In case of fatigue life, number of complete continuous tows in samples had an exponential relationship with the fatigue life capacity for each tow starting with 16458 cycle for single tow for 0 degrees and 23384, 5141, 4115, 3764, 2576 cycles per tows for 5, 10, 15 and 25 degrees. Coupons with 6 and 7 tows had high number of fatigue cycles without failure when compared to 5 and 4 tows. Consistency in fatigue behaviors of materials are difficult, but from the data collected it is evident that number of continuous tows present in the coupons impacts the fatigue life.

The percentage reduction in compressive strength between 0 degree and 25 degree shifted fabric was 40%. Between two consecutive shifted fabric [0-5, 5-10, 10-15, 15-20, 20-25], the percentage reduction in compressive values were 6.5%, 17.5%, 12.7% and 12.1% respectively. It was also clearly found from the *table 02* and *figure 34* that the trial 1 and trial-2 coupons had almost same properties with a standard deviation of 5.77 MPa in the compressive strength. The reduction in coupon thickness influences compressive strength of the fabric and a graphical representation of reduction in coupon thickness versus reduction in compressive strength is shows in the *figure 35*.

Straight coupons cut from the shifted samples are also put to the same compressive tests [*Table 05*] and the percentage reduction in compressive force between the coupons [0-5, 5-10, 10-15, 15-20, 20-25] are 5%,1.7%,3.5% and 1.8% which makes it all together of 11.6% reduction in property. The average compressive values of shifted fabric cut from shifted samples was compared to straight fabric cut out from shifted sample. From *table 01*, it is evident that the fabric with shift angles more than 10 degrees deteriorates mechanical properties largely. *Table 01* shows that the compressive strength for shifted and straight fabric with 0, 5 and 10 degree remained same for all of them except 5 degree had a 7 MPa higher value for the shifted fabric. This value is negligible when compared to 15, 20 and 25 degree where the difference are 58, 85 and 113 MPa. Hence there is reduction in mechanical properties for the fabrics when shifted above 10 degrees.

Table 01: Strength Summary for the straight coupon cut from shifted sample

Shift Angle	Ultimate breaking Load [Kgf]	Compressive Strength [MPa]
0	3276	430
5	3264	428
10	2677	401
15	2582	395
20	2356	382
25	2230	374

Table 02: Compression test result for shifted coupon from two trials

Applied Shift Angle	Measured shift angle	% Spring back	No. of continuous tows remained in sample	Average coupon Thickness [cm]	Ultimate breaking Load – Coupon 1 [Kg]	Ultimate breaking Load – Coupon 2 [Kg]	Average Compressive Load [Kg]	Compressive Strength - Trial 1 [MPa]	Compressive Strength - Trial 2 [MPa]	Average Compressive Strength [MPa]	Compressive strength acting per tow [MPa]
0	0	0	7	0.3	-	-	3276	-	-	437	62
5	4	20	6	0.3	3343	3350	3346	446	447	447	74
10	8	20	6	0.27	2751	2721	2735	408	403	406	68
15	12	20	5	0.26	2351	2108	2229	362	324	343	69
20	15	25	5	0.25	1866	1816	1841	299	291	295	59
25	19	24	4	0.24	1574	1544	1559	262	257	260	65

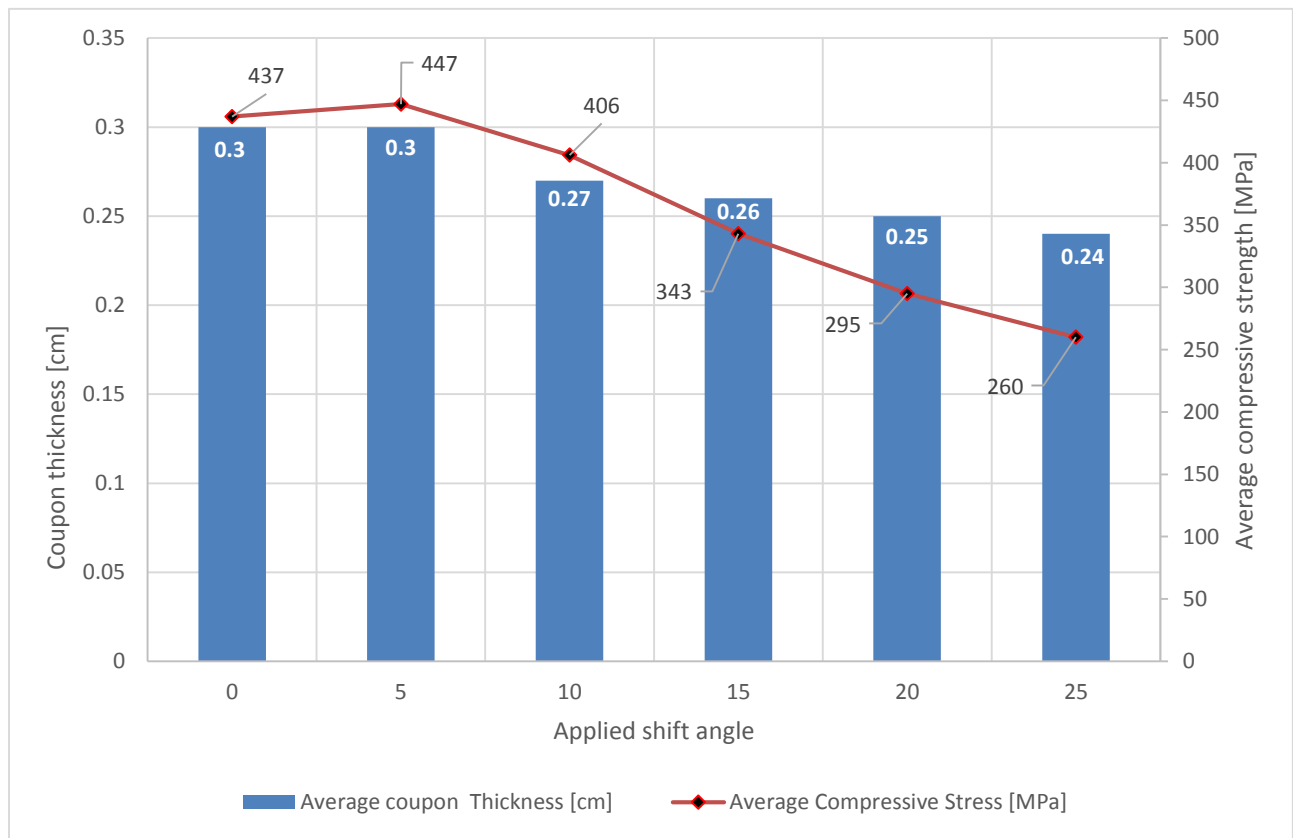


Figure 32: A graphical representation showing varying coupon thickness influencing compressive force

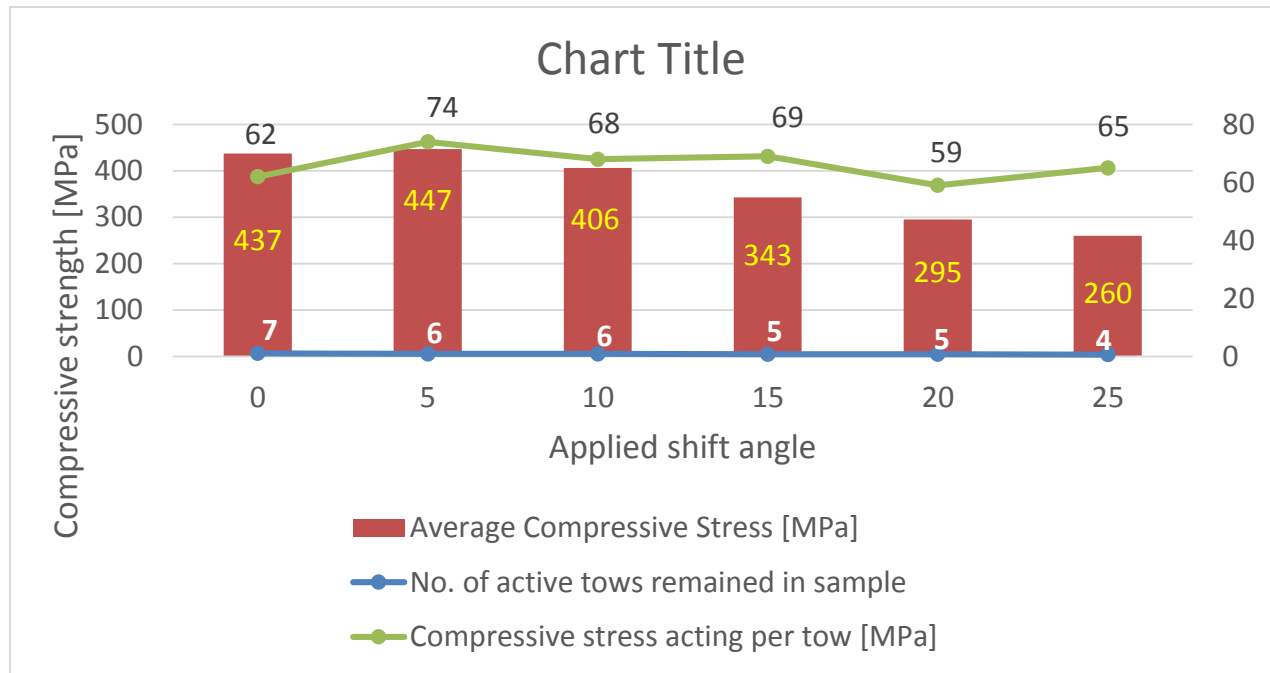


Figure 33: A comparison between tows in a shifted coupon versus average compressive strength of shifted coupon - Data from table 02.

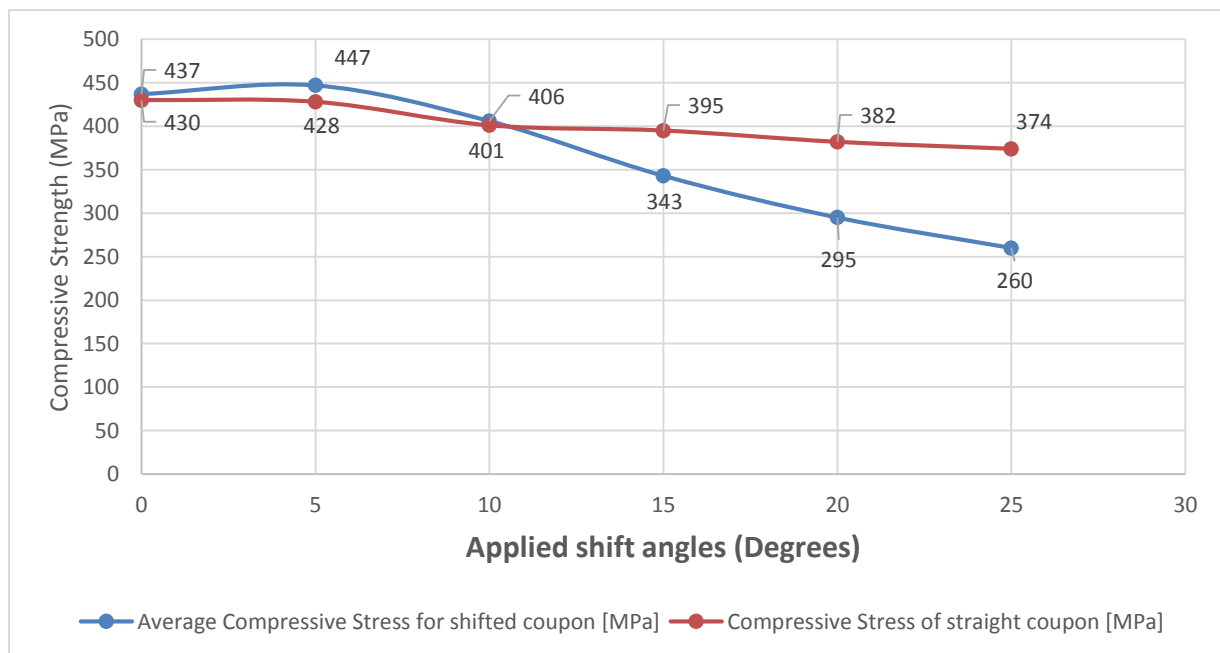


Figure 34: Compression results of the Straight Coupon cut from the Shifted sample Vs Shifted Coupons cut from Shifted samples

Data from the *table 02* shows us that the coupons with shift angles above 10 degree have reduced mechanical properties. One of the major cause of this effects is due to the strength concentration in the shifted region. Coupons with shift angle above 10 degrees are prone form a small bump in the samples which is theoretical out-of-plane wave. The out-of-plane waviness, tow thinning and in-plane waviness all together causes strength concentration in the fabric coupons. Since this strength concentration reduces the mechanical properties of the fabric, it is essential to model the coupon and simulate the strength concentration acting on the shifted coupon.

Two coupons with out-of-plane waviness, each the varying radius of curvature were analyzed by applying same compressive force. The analysis was replicated just like the compressive tests done in lab. A 6000 psi [41 MPa] compression force were applied to both the models created. When a rectangular cross sectioned beam is compressed vertically, it buckles. Since the sample had a slight bump in the center due to in-plane waves, our fabric had the highest strength concentration in the same location. Both the samples showed the strength concentration highest at the out-of-plane waviness region (curved region), but the strength concentration was higher for the samples with higher out-of-plane waviness [*Figure 41*] compared to samples with lower out-of-plane waviness [*Figure 40*].

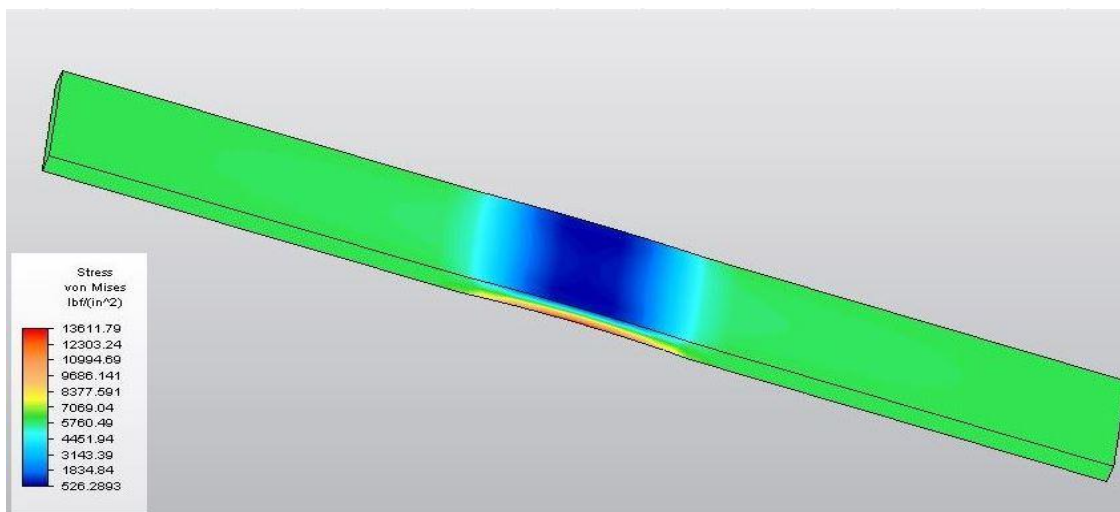


Figure 35: Stress Analysis on a coupon with lower out-of-plane [7 inch radius of curvature] waviness.

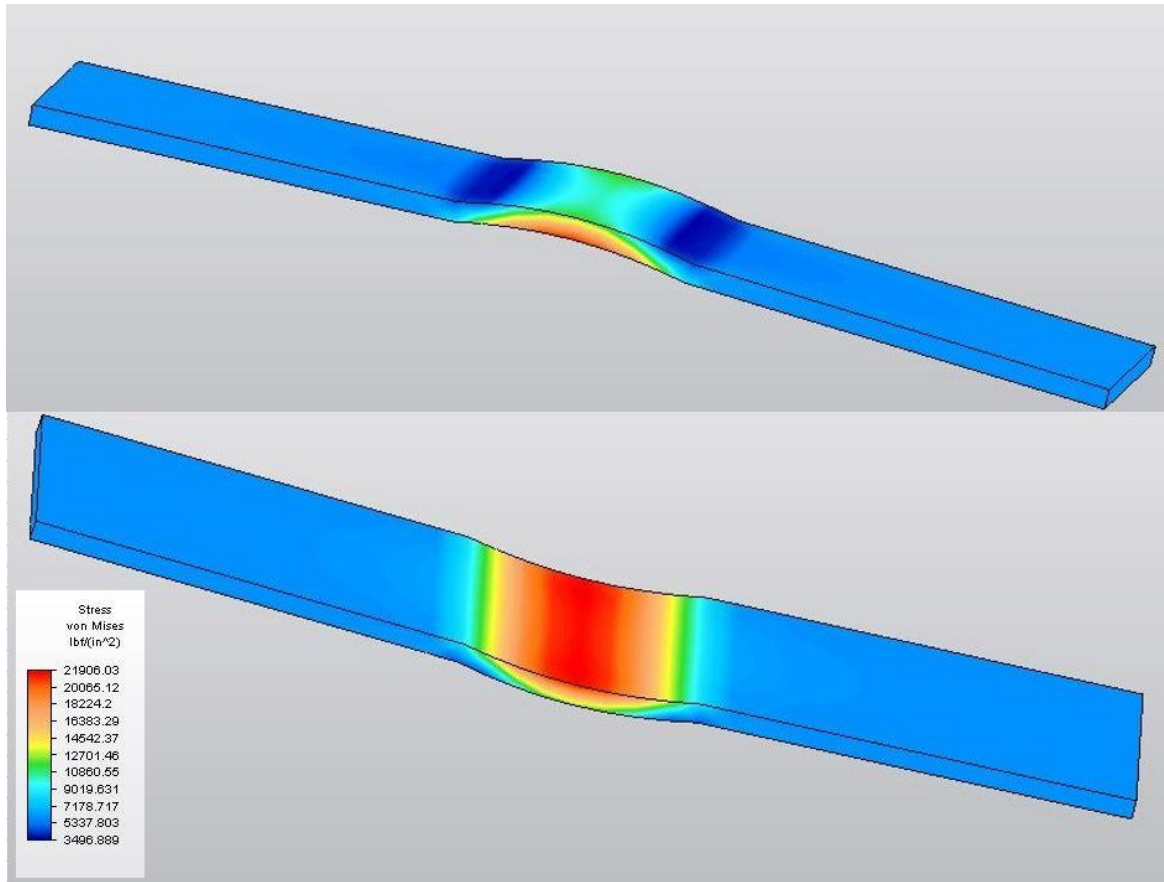


Figure 36: Stress Analysis on a coupon with higher out-of-plane [4 inch radius of curvature] waviness

The understanding of fabric behavior on shifting was backed up with data collected by fatigue tests. All the coupons for fatigue testing were subjected to 85% compressive load. The compressive testing was done prior to the fatigue testing to get load to set the load for fatigue testing. When one of the fatigue tests cycle trial for 0 and 5 degree refused to show any sign of wear and tear at 130 thousand cycles, the load for fatigue testing cycle was increased to 90%. It is very evident from the data in *table 06* that coupons with lower shift angles sustained a more number of cycles and the samples with higher shift angle started failing with lesser number of cycles at same 85% load. Number of sample size of 2 per shift angle for the fatigue tests are not enough to make a conclusion on the fabric properties on shift. This study was limited to 2 samples per shift angles due to the time availability.

Table 03: Fatigue testing results of the samples- Load applied and number of cycles sustained.

	Trial 1		Trial 2		
Shift Angle	Applied Force [Kgf]	Number of Cycles	Applied Force [Kgf]	Number of Cycles	Average Number of Cycles
0 **	2785	89,873	2785 then 2948	136,718 then 3832	115,212
5 **	2844 then 3011	230,725 then 2,150	2844	47,741	140,308
10	2325	32,163	2325	29,533	30,848
15	1895	8,947	1895	32,173	20,560
20	1565	18,717	1565	18,929	18,823
25	1325	16,762	1325	3,846	10,304

Note **: Coupons of 0 and 5 degree did not break for a longer number of fatigue cycle at 85% load. Therefore those coupons were ran second time at 90% of the load.

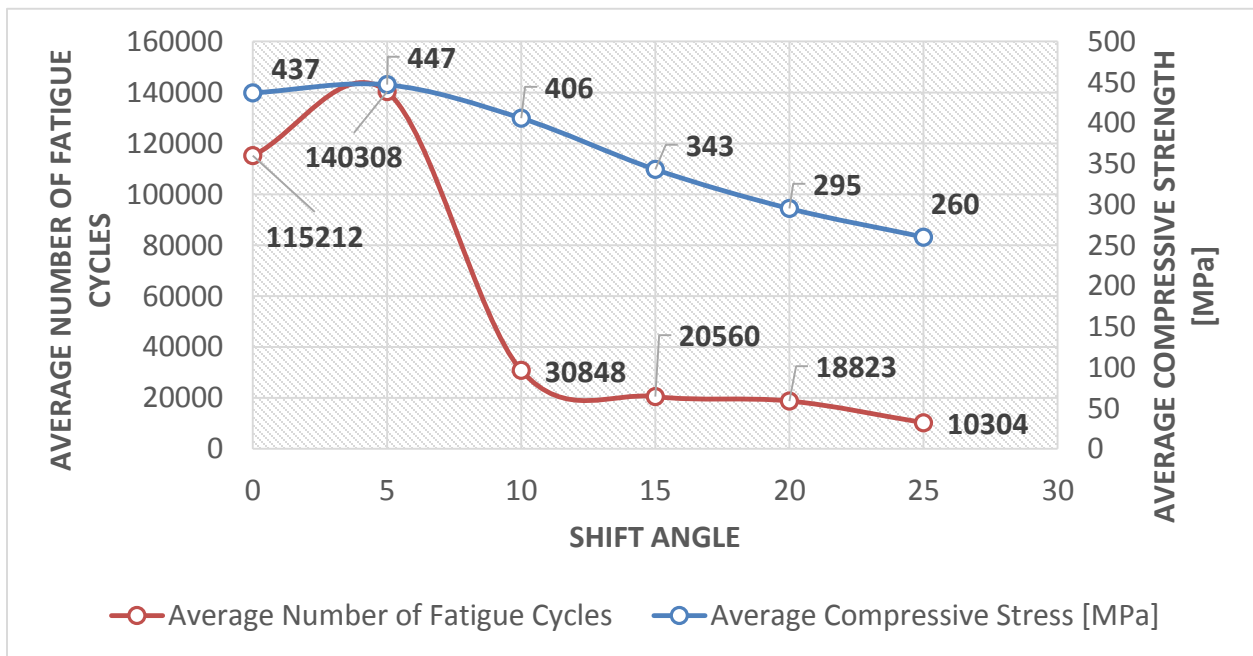


Figure 38: A comparison between Average Compressive Strength versus shift angle and Average Fatigue Cycles versus shift angle

Chapter 6: Conclusions and Future Work

The study provides insights into the effects of shifting which results in in-plane waviness followed by out-of-plane waviness in unidirectional fabric. The study focused on various shift angles on the fabric and its intensity of impact on final mechanical properties. The study suggests the potential issues with the fabric shift deformation. The samples were all prepared and cut in the same manner, but the final thickness of the samples varied depending on the shift angles. Thickness varied due to the fiberglass overlapping from shifting creating tow thinning. The out of plane waviness on the fabric causes high strength concentration to the region and also a thickness variation ranging from .23 - .30 cm. The out-of-plane waviness is also considered as a pre-buckled shape. The strength concentrated in that region expedites the buckling effect in fatigue or compression tests

For an unaltered fabric, the fibers are oriented in unidirectional way and there are no restrictions to the flow of resin. Here the tows are not closely packed and there is least resistance to resin flow. When a shift is introduced to the fabric, an obstruction is created in the path of resin flow. Tow thinning at the shifted region resulted in difference in creating resistance to resin flow by 5-7% of time in out-of-plane wave region. Due to tow thinning, tows are packed with more density in the shifted region, so the resin flows with normal flow rate until the shift location and pause for some time in the shifted location. The resin accumulates in that region until the resin cannot stay in that region anymore and then it starts flowing again in the shifted region. The resin flow is comparatively slow in the shifted region than the straight region, but this does not result in any low resin areas though.

Reviewing all the data collected from the tests, we can conclude that the fabrics shifted up to 10 degrees does not affect the properties. In practical application of wind turbine manufacturing, the fabrics are not shifted beyond 8 degrees. In that case, we can assume the fabric shifting machine is safe for the wind turbine manufacturing applications without

compromising the quality. It was also confirmed that there is no significant difference between straight coupons and Shifted coupons for 0, 5 and 10 degree shift angles. These findings are significant in terms of machine design and utilization. This will also help for further research and improvement in the related field of fabric layup automation.

Future work:

This research work was done to the best possible way, but still there are few things that need to be taken into consideration for future research work. In the entire research the samples were made by stacking 4 layers of shifted fabric over each other to make the samples. But in actual application, these fabrics are not stacked exactly over each other, but are stacked with offsets. Studies need to be done to investigate how samples created with offset performs with the mechanical tests. Another important factor of fabric *spring-back* needs to be included in future studies. For taking *spring-back* into account, a detailed model and study need to be prepared on the fabric *spring-back* prior to starting the actual study. Over-shifting could be a possible way to overcome the *spring-back* effect. Since we noticed the fabrics are straightening about 21.8% after the shifting, these spring back can be compensated in the input angle. Different types of fabric with different shift angles behave differently, so the study needs to be intense to characterize it.

Moving the shifted fabric from the machine table to the infusion table was challenging. This could be a small source of variability in the fabric deformation but need to be handled better. A provision to infuse the fabric in the machine table would be the best chance to overcome this variability. This not only reduces the effects of fabric displacement, but also saves time to get the original layup orientation from the shift machine. This also reduces the variability and will gain better control of the fabric and samples in terms of thickness, density and fabric layup position.

More detailed study of the tow thinning of the fabric from the shifting needs to be done. The tow thinning takes place in the point of clamping on the fabric. In order for this study, radiography techniques must be done on the shifted fabric to study the tow thinning more in details and focus more in the point of clamping region. Radiography image gives a better understanding of tow breakage and internal link breakage and the understandings can be

backed up by conducting study in microstructural level. This will help in expanding our knowledge of in-plane waviness caused by the shifting mechanism. With the help of this, the internal features of the materials can be better characterized. The knowledge can be made more concrete by including more of nondestructive evaluation to the samples. This can be achieved easily by characterizing the materials with ultrasonic wave velocity analysis that help in defect analysis and inclusions within the fabric.

References

1. M. J. Shuart, "Failure of Compression-Loaded Multidirectional Composite Laminates," AIAA Journal, Vol.27, No.9, September 1989, pp.1274-1279.
2. Lei Wang, "Effects of In-Plane Fiber Waviness on the Static and Fatigue Strength of Fiberglass" Masteral Thesis, Montana State University, 2001.
3. Potter, K. "The influence of accurate stretch data for reinforcements on the production of complex structural mouldings Part 1. Deformation of aligned sheets and fabrics." Composites 10 (1979): 161-67.
4. Darrell P. "Compression Strength of Carbon fiber Laminates Containing Flaws with fiber waviness" 42nd AIAA Aerospace Sciences Meeting and Exhibit (2004), pp. 54-63 Key: citeulike:6792719
5. Advani, S.G., Bruschke, M.V. and Pamas, R., Resin transfer molding, Chapter 12. In Flow and Rheology in Polymeric Composites Manufacturing, ed. S.G. Advani, Elsevier Publishers, Amsterdam, 1994
6. S. Bickerton et al. "Investigation of draping and its effects on the mold filling process during manufacturing of a compound curved composite part" Journal of Composite Materials March 2011 vol. 45 no. 6 695-716
7. Zhu, B., T. Yu, and X. Tao. "An experimental study of in-plane large shear deformation of woven fabric composite." Composites Science and Technology 67 (2007): 252-61.
8. D. Adams, J. Reinforced Plastics and Composites, 12, April 1993, pp. 415-429.
9. N. A. Fleck, T. W. Clyne, M. P. F. Sutcliffe and A. Kelly, "A Fundamental Study of the Compressive Failure of Polymer Matrix composites," EPSRC Reports, EPSRC Grant GR/L19812.
10. Kantharaju "Analysis of fiber waviness in laminated composites subjected to compressive loads" Thesis, Visvesvaraya Technological University, 2007.
11. Rosen B.W., "Mechanics of Composite Strengthening", Chapter 3, American Society of Metal, 1965
12. Fleck N.A., Bundiansky B., "Compressive Failure of Fiber Composites", Journal of the Mechanics and Physics of Solids, Vol. 41, Issue 3, pp 183-211,1993.
13. Hahn, H. T.; Turkgenc, Ozgur "The Effect of Loading Parameters on Fatigue of Composite Laminates: Part IV Information Systems" Part II, DOT/FAA/AR-96/76, July

1997.

14. Stinchcomb, W.W. and C.E. Bakis, "Fatigue Behavior of Composite Laminates," *Fatigue of Composite Materials*, Edited by K.L. Reifsnider, Elsevier Sc. Publishers, 1990, pp. 105-180.
15. Bogetti T.A., Gillespie J.W., Lamontia M.A., "Influence of Ply Waviness on the Stiffness and Strength Reduction on Composite Laminates," *Journal of Thermoplastic Composite Materials*, Vol. 5, pp 344-369, October 1992.
16. Joyce P., Moon T.J., "Compression Strength Reduction in Composites with In Plane Fiber Waviness," *Composite Materials: Fatigue and Fracture*, Vol. 7, pp 76-96, 1998.
17. Hsiao H.M., Daniel I.M., "Effect of Fiber Waviness on Stiffness and Strength Reduction of Unidirectional Composites under Compressive Loading," *Composites Science and Technology*, Vol. 56, pp 581-593, February 1996.
18. Hsiao H.M., Daniel I.M., "Nonlinear Elastic Behavior of Unidirectional Composites with Fiber Waviness under Compressive Loading," *Journal of Engineering Materials and Technology*, Vol. 118, pp 561-570, October 1996.
19. Wisnom M.R., Atkinson J.W., "Fiber Waviness Generation and Measurement and Its Effect on Compressive Strength," *Journal of Reinforced Plastics and Composites*, Vol. 19, Issue 2, pp 96-110, 2000.
20. Chun H.J., Shin J.Y., Daniel I.M., "Effects of Material and Geometric Nonlinearities on the Tensile and Compressive behavior of Composite Materials with Fiber Waviness," *Composites Science and Technology*, Vol. 61, pp 125-134, 2001.
21. Fleck N.A., Liu D., "Microbuckle Initiation from a Large Amplitude Fiber Waviness in a Composite under Compression and Bending," *European Journal of Mechanics – A/Solids*, Vol. 20, Issue 1, pp 23-37, 2001.
22. Daniel I.M., Ishai O., "Engineering Mechanics of Composite Materials", Second Edition, Oxford University Press, 2006
23. Garnich M.R., Karami G., "Finite Element Micromechanics for Stiffness and Strength of Wavy Fiber Composites," *Journal of Composite Materials*, Vol. 38, Issue 4, pp 273-292, 2004.
24. Robertson, R.E., T.-J. Chu, R.J. Gerard, J.-H. Kim, M. Park, H.-G. Kim, and R.C. Peterson. "Three-dimensional fiber reinforcement shapes obtainable from flat, bidirectional fabrics without wrinkling or cutting. Part 1. A single four-sided pyramid." *Composites Part A: Applied Science and Manufacturing* 31 (2000): 703-15.

25. Mills, A. "Automation of Carbon Fiber Preform Manufacture for Affordable Aerospace Applications." *Composites Part A: Applied Science and Manufacturing* 32.7 (2001): 955-62.
26. Hancock, S., and K. Potter. "The Use of Kinematic Drape Modelling to Inform the Hand Lay-up of Complex Composite Components Using Woven Reinforcements." *Composites Part A: Applied Science and Manufacturing* 37.3 (2006): 413-22. Print.
27. Mohammed, U., C. Lekakou, and M. Bader. "Experimental Studies and Analysis of the Draping of Woven Fabrics." *Composites Part A: Applied Science and Manufacturing* 31.12 (2000): 1409-420.
28. Buckingham, R., and G. Newell. "Automating the Manufacture of Composite Broadgoods." *Composites Part A: Applied Science and Manufacturing* 27.3 (1996): 191-200.
29. Shirinzadeh, B. "Fabrication Process of Open Surfaces by Robotic Fiber Placement." *Robotics and Computer-Integrated Manufacturing* 20.1 (2004): 17-28.
30. Kordi, Tarsha M., M. Husing, and B. Corves. "Development of a Multifunctional Robot End-Effector System for Automated Manufacture of Textile Preforms." *Proc. of 2007 IEEE/ASME International Conference on Advanced Intelligent Mechatronics, AIM, Switzerland, Zurich*. Piscataway, NJ: Institute of Electrical and Electronics Engineers, 2007.
31. Salkind, J. J., "Fatigue of Composites," *Composite Materials: Testing and Design (Second Conference)*, ASTM STP 497, American Society for Testing and Materials, 1972, pp. 143-169.
32. Miner, M. A. "Cumulative Damage in Fatigue." *Applied Mechanics* 12.A (1945): 59-64.
33. Creed, Jr., Richard Francis. *High Cycle Tensile Fatigue of Unidirectional Fiberglass Composite Tested at High Frequency*. Thesis. Montana State University, 1993. Print.
34. Wahl, N.W., Samborsky, D.D., Mandell, J.F., and Cairns, D.S., "Spectrum Fatigue Lifetime and Residual Strength for Fiberglass Laminates in Tension," 2001 ASME Wind Energy Symposium, AIAA-2001-0025, ASME/AIAA. (2001)
35. Mandell, J. F., Reed, R. M., and Samborsky, D. D. "Fatigue of Fiberglass Wind Turbine Blade Materials" SAND92-7005, Sandia National Laboratories, 1992
36. Wang, Lei. "Effects of In-Plane Fiber Waviness on the Static and Fatigue Strength of Fiberglass". Thesis. Montana State University, 2001.

37. Hahn HT, Kim RY. Fatigue behaviour of composite laminate. *Composite Materials* 1976;10:156±80
38. Magnussen, C. "A fabric deformation methodology for the automation of fiber reinforced polymer composite manufacturing." Thesis. Iowa State University, 2011. Ames: ProQuest/UMI, 2011.
39. J.F. Mandell, D.D. Samborsky, and L. Wang, Proc. 48th International SAMPE Symposium, L.J. Colen, C.L. Ong, C. Arendt, eds., Vol. 48, SAMPE, Covina, CA, 2003, pp.2653-2666.
40. Riddle T. W., Cairns D. S., Nelson J. W., " Characterization of Manufacturing Defects Common to Composite Wind Turbine Blades: Flaw Characterization"
41. Riddle T. W., Cairns D. S., Nelson J. W., " Manufacturing Defects Common to Composite Wind Turbine Blades: Effects of Defects "
42. B. H. Le Page, C. I. C. Manger, F. J. Guild, S. L. Ogin, and P. A. Smith, " Modelling effect of layer shift on properties of woven fabric composites
43. Reifsnider, K. L., "Damage and Damage Mechanics (Chapter 2)," *The Fatigue Behavior of Composite Materials*, K. L. Reifsnider, Ed., Elsevier (1990), pp. 11-77.
44. Wade Johanns., "The effect of tow grouping resolution on shearing deformation of unidirectional non-crimp fabric".
45. ASTM D3410/D3410M., " Standard Test Method for Compressive Properties of Polymer Matrix Composite Materials with Unsupported Gage Section by Shear Loading"
46. Wollner, Benjamin [2011]. Development of a fabric winding system for the automated manufacture of prefabricated wind turbine blade roots. Master of Science. Iowa State University. United States
47. Ruth DE and Mulgaonkar P. Robotic layup of prepreg composite plies. Proceedings of IEEE international conference on robotics and automation, Cincinnati, OH (May 13-18, 1990) 1296-1300.
48. Sarhadi M. Automated lay-up of non-rigid fabrics. Proceedings of the Manufacturing Technology Update, IEE; June 1993.

Appendix A

TABLE 2 Compression Specimen Geometry Recommendations

Fiber Orientation	Width, mm [in.]	Gage Length, mm [in.]	Tab Length, mm [in.]	Overall Length, mm [in.]	Tab Thickness, mm [in.]
0°, unidirectional	10 [0.5]	10–25 [0.5–1.0]	65 [2.5]	140–155 [5.5–6.0]	1.5 [0.06]
90°, unidirectional	25 [1.0]	10–25 [0.5–1.0]	65 [2.5]	140–155 [5.5–6.0]	1.5 [0.06]
Specially orthotropic	25 [1.0]	10–25 [0.5–1.0]	65 [2.5]	140–155 [5.5–6.0]	1.5 [0.06]

TABLE 3 Minimum Required Specimen Thickness (mm [in.])

Minimum Required Thickness (mm [in.]) for 10-mm [0.5-in.] Gage Length						
Longitudinal Modulus, GPa [Msi]	Expected Compression Strength, F^{cu} , MPa [ksi]					
	300 [50]	600 [100]	900 [150]	1200 [200]	1500 [250]	1800 [300]
25 [5]	1.27 [0.058]	1.89 [0.087]	2.45 [0.114]	3.02 [0.142]	3.64 [0.174]	4.36 [0.214]
50 [7]	1.00 [0.049]	1.33 [0.074]	1.73 [0.096]	2.14 [0.120]	2.58 [0.147]	3.08 [0.180]
75 [10]	1.00 [0.041]	1.09 [0.062]	1.41 [0.081]	1.74 [0.101]	2.10 [0.123]	2.52 [0.151]
100 [15]	1.00 [0.040]	1.00 [0.050]	1.22 [0.066]	1.51 [0.082]	1.82 [0.101]	2.18 [0.123]
200 [20]	1.00 [0.040]	1.00 [0.044]	1.00 [0.057]	1.07 [0.071]	1.29 [0.087]	1.54 [0.107]
300 [30]	1.00 [0.040]	1.00 [0.040]	1.00 [0.047]	1.00 [0.058]	1.05 [0.071]	1.26 [0.087]
400 [50]	1.00 [0.040]	1.00 [0.040]	1.00 [0.040]	1.00 [0.045]	1.00 [0.055]	1.09 [0.068]
500 [70]	1.00 [0.040]	1.00 [0.040]	1.00 [0.040]	1.00 [0.040]	1.00 [0.047]	1.00 [0.057]
Minimum Required Thickness (mm [in.]) for 20-mm [0.75-in.] Gage Length						
Longitudinal Modulus, GPa [Msi]	Expected Compression Strength, F^{cu} , MPa [ksi]					
	300 [50]	600 [100]	900 [150]	1200 [200]	1500 [250]	1800 [300]
25 [5]	2.53 [0.087]	3.77 [0.131]	4.90 [0.171]	6.04 [0.214]	7.28 [0.262]	8.72 [0.320]
50 [7]	1.79 [0.074]	2.67 [0.111]	3.46 [0.145]	4.27 [0.180]	5.15 [0.221]	6.17 [0.271]
75 [10]	1.46 [0.062]	2.18 [0.092]	2.83 [0.121]	3.49 [0.151]	4.21 [0.185]	5.04 [0.226]
100 [15]	1.27 [0.050]	1.89 [0.075]	2.45 [0.099]	3.02 [0.123]	3.64 [0.151]	4.36 [0.185]
200 [20]	1.00 [0.044]	1.33 [0.065]	1.73 [0.086]	2.14 [0.107]	2.58 [0.131]	3.08 [0.160]
300 [30]	1.00 [0.040]	1.09 [0.053]	1.41 [0.070]	1.74 [0.087]	2.10 [0.107]	2.52 [0.131]
400 [50]	1.00 [0.040]	1.00 [0.041]	1.22 [0.054]	1.51 [0.068]	1.82 [0.083]	2.18 [0.101]
500 [70]	1.00 [0.040]	1.00 [0.040]	1.10 [0.046]	1.35 [0.057]	1.63 [0.070]	1.95 [0.086]
Minimum Required Thickness (mm [in.]) for 25-mm [1.0-in.] Gage Length						
Longitudinal Modulus, GPa [Msi]	Expected Compression Strength, F^{cu} , MPa [ksi]					
	300 [50]	600 [100]	900 [150]	1200 [200]	1500 [250]	1800 [300]
25 [5]	3.17 [0.116]	4.72 [0.174]	6.12 [0.228]	7.55 [0.285]	9.10 [0.349]	10.91 [0.427]
50 [7]	2.24 [0.098]	3.33 [0.147]	4.33 [0.193]	5.34 [0.241]	6.44 [0.295]	7.71 [0.361]
75 [10]	1.83 [0.082]	2.72 [0.123]	3.53 [0.161]	4.36 [0.201]	5.26 [0.247]	6.30 [0.302]
100 [15]	1.58 [0.067]	2.36 [0.101]	3.06 [0.132]	3.77 [0.164]	4.55 [0.201]	5.45 [0.247]
200 [20]	1.12 [0.058]	1.67 [0.087]	2.16 [0.114]	2.67 [0.142]	3.22 [0.174]	3.86 [0.214]
300 [30]	1.00 [0.047]	1.36 [0.071]	1.77 [0.093]	2.18 [0.116]	2.63 [0.142]	3.15 [0.174]
400 [50]	1.00 [0.040]	1.18 [0.055]	1.53 [0.072]	1.89 [0.090]	2.28 [0.110]	2.73 [0.135]
500 [70]	1.00 [0.040]	1.05 [0.047]	1.37 [0.061]	1.69 [0.076]	2.04 [0.093]	2.44 [0.114]